doi.org/10.26434/chemrxiv.12674345.v1

Molecular Modeling of Structures and Interaction of Short Peptides and Sortase Family Protein of Enterococcus Faecalis: Basis for Developing Peptide-Based Therapeutics Against Multidrug Resistant Strains

Muthusaravanan S, Ram Kothandan, Kumaravel Kandaswamy, Cashlin Anna Suveetha Gnana Rajan, Janamitra Arjun, Rejoe Raymond

Submitted date: 20/07/2020 • Posted date: 21/07/2020

Citation information: S, Muthusaravanan; Kothandan, Ram; Kandaswamy, Kumaravel; Gnana Rajan, Cashlin Anna Suveetha; Arjun, Janamitra; Raymond, Rejoe (2020): Molecular Modeling of Structures and Interaction of Short Peptides and Sortase Family Protein of Enterococcus Faecalis: Basis for Developing Peptide-Based Therapeutics Against Multidrug Resistant Strains. ChemRxiv. Preprint.
https://doi.org/10.26434/chemrxiv.12674345.v1

The Enterococcus faecalis (E. faecalis) infection starts with initial adhesion to a host cell or abiotic surface by multiple adhesions on its cell membrane. The pathogenicity is due to virulence factors SrtA, SrtC, EbpA, EbpB, EbpC, and Aggregation Substance. E. faecalis developed resistance to the majority of standard therapies. Additionally, a notable key feature of E. faecalis is its ability to form biofilm in vivo. E. faecalis strains show resistance to aminoglycosides and β-lactam antibiotics with different degree of susceptibility. Sortases (SrtA and SrtC) are enzymes spatially localized at the septal region in majority of gram-positive bacteria during the cell cycle, which in-turn plays an important role in proper assembling of adhesive surface proteins and pilus on cell membrane. The studies have also proved that the both SrtA and SrtC were focally localized in E. faecalis and essential for efficient bacterial colonization and biofilm formation on the host tissue surfaces Using homology modeling and protein-peptide flexible docking methods, we report here the detailed interaction between peptides and EfSrt (Q836L7) enzyme. Plausible binding modes between EfSrt and the selected short biofilm active peptides were revealed from protein-peptide flexible docking. The simulation data further revealed critical residues at the complex interface and provided more details about the interactions between the peptides and EfSrt. The flexible docking simulations showed that the peptide-EfSrt binding was achieved through hydrogen bonding, hydrophobic, and van der Waals interaction. The strength of interactions between peptide-EfSrt complexes were calculated using standard energy calculations involving non-bonded interactions like electrostatic, van der Waals, and hydrogen bonds.

File list (2)

Manuscript_SrtAEF.docx (3.23 MiB) view on ChemRxiv • download file

Molecular modeling of structures and interaction of short peptides and Sortase family protein of *Enterococcus faecalis*: Basis for developing peptide-based therapeutics against multidrug resistant strains

Muthusaravanan Sivaramakrishnan [a,b], Kumaravel Kandaswamy [b], Cashlin Anna Suveetha Gnana Rajan [a], Janamitra Arjun [a], Rejoe Raymond [a] and Ram Kothandan *[a].

[a]Bioinformatics Laboratory, Department of Biotechnology, Kumaraguru College of Technology, Coimbatore, Tamil Nadu, India.

[b]Laboratory of Molecular Biology and Genetic Engineering, Department of Biotechnology, Kumaraguru College of Technology, Coimbatore, Tamil Nadu, India.

Graphical abstract

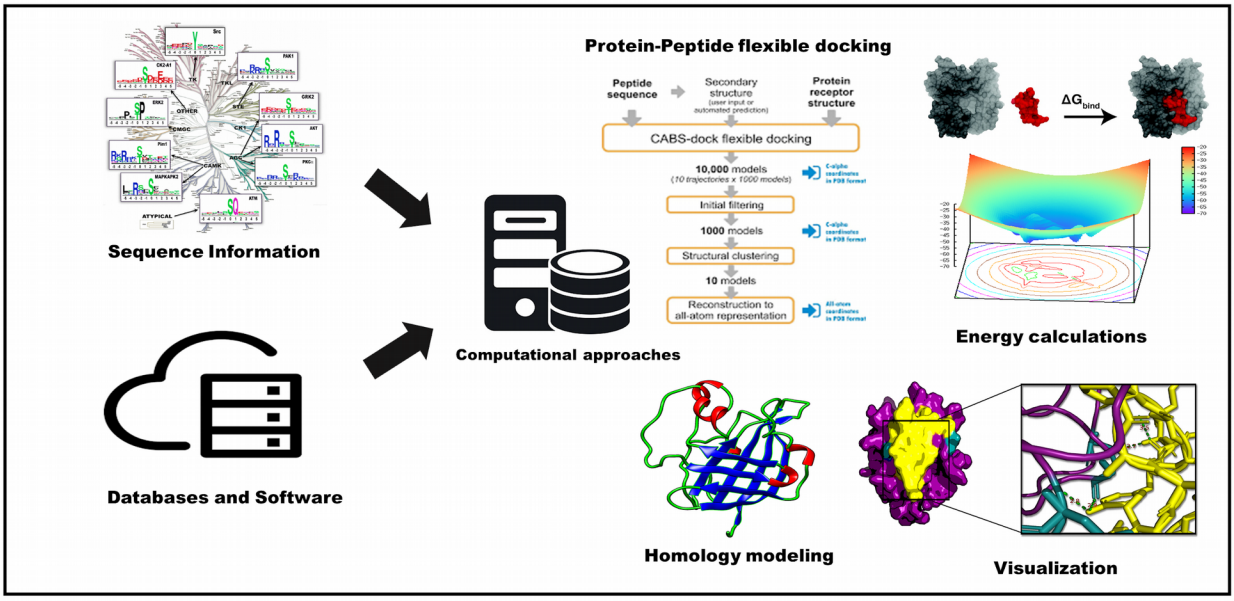

Abstract

The *Enterococcus faecalis* (*E. faecalis*) infection starts with initial adhesion to a host cell or abiotic surface by multiple adhesions on its cell membrane. The pathogenicity is due to virulence factors SrtA, SrtC, EbpA, EbpB, EbpC, and Aggregation Substance. *E. faecalis* developed resistance to the majority of standard therapies. Additionally, a notable key feature of *E. faecalis* is its ability to form biofilm *in vivo*. *E. faecalis* strains show resistance to aminoglycosides and β-lactam antibiotics with different degree of susceptibility. Sortases (SrtA and SrtC) are enzymes spatially localized at the septal region in majority of gram-positive bacteria during the cell cycle, which in-turn plays an important role in proper assembling of adhesive surface proteins and pilus on cell membrane. The studies have also proved that the both SrtA and SrtC were focally localized in *E. faecalis* and essential for efficient bacterial colonization and biofilm formation on the host tissue surfaces Using homology modeling and protein-peptide flexible docking methods, we report here the detailed interaction between peptides and *Ef*Srt (Q836L7) enzyme. Plausible binding modes between *Ef*Srt and the selected short biofilm active peptides were revealed from protein-peptide flexible docking. The simulation data further revealed critical residues at the complex interface and provided more details about the interactions between the peptides and *Ef*Srt. The flexible docking simulations showed that the peptide-*Ef*Srt binding was achieved through hydrogen bonding, hydrophobic, and van der Waals interaction. The strength of interactions between peptide-*Ef*Srt complexes were calculated using standard energy calculations involving non-bonded interactions like electrostatic, van der Waals, and hydrogen bonds.

Keywords: Drug resistance, *E. faecalis*, Biofilm, Sortase enzymes, protein-peptide docking, standard energy calculations.

Introduction

Enterococcus faecalis (*E. faecalis*) is a gram positive commensal opportunistic pathogen, responsible for various hospital acquired infections [1]. *E. faecalis* strains can overcome several harsh environments by forming biofilms on host tissues and abiotic surfaces. Furthermore, *E. faecalis* harbors virulence proteins on its cell membrane and an antimicrobial peptide sensing system to protect them against antibiotics and cationic antimicrobial peptides, respectively [2].

E. faecalis causes over 18,000 deaths a year, making it an important pathogen to be studied. Over the past three decades, various research groups have studied *E. faecalis* strains intensively to explore its interaction with hosts, determine the basis of pathogenesis, and virulence proteins localization to find effective treatment strategies [3]. However, currently there is no effective drug available for its prevention and infections still exist. *E. faecalis* is also capable of forming biofilms and responsible for various biofilm-associated infections such as Urinary Tract Infection (UTI), surgical wound infection, and nosocomial bacteremia [4]. The mature biofilm showed high tolerance to antibiotics than the planktonic bacteria, even at higher concentrations of 10–1000 times [5]. The *E. faecalis* infection starts with initial adhesion to a host cell or abiotic surface by multiple adhesions on its cell membrane. The pathogenicity is due to virulence factors SrtA, SrtC, EbpA, EbpB, EbpC, and Aggregation Substance [6]. *E. faecalis* developed resistance to the majority of standard therapies [7]. Additionally, a notable key feature of *E. faecalis* is its ability to form biofilm [8]. *E. faecalis* strains show resistance to aminoglycosides and β-lactam antibiotics with different degree of susceptibility [9]. It shows moderate resistance to former due to its low permeability through the cell wall (aminoglycoside molecules are larger) and intrinsic resistance to later due to over-expression of penicillin binding proteins. The antibiotics available today were not effective against Multiple Drug Resistance (MDR) enterococcal infections such

endocarditis or bacteremia along with neutropenia [10]. The antibiotics combinations such as ciprofloxacin with ampicillin, novobiocin with doxycycline, and penicillin with vancomycin were used to treat enterococcal infections [11], but efficiency of this treatment remains doubtful.

Sortases (SrtA and SrtC) are enzymes spatially localized at the septal region in majority of gram-positive bacteria during the cell cycle, which in-turn plays an important role in proper assembling of adhesive surface proteins and pilus on cell membrane [12]. The studies have also proved that the both SrtA and SrtC were focally localized in *E. faecalis* and essential for efficient bacterial colonization and biofilm formation on the host tissue surfaces [13]. The Sortase mutants produce defective pili and found to be less virulent than the wild type strain [14]. The Spatial localization of virulence factors and Sortase mediated pilus assembly in *Enterococcus faecalis* was illustrated in **Figure 1**.

Recent studies on antimicrobials suggest that peptides as possible drug candidates and to overcome drug resistance in *E. faecalis*. Moreover, studies have also shown that this species can rapidly acquire resistance even to cationic antimicrobial peptides such as β-beta defensins [15]. Multiple peptide resistance Factors (mprF1 and mprF2) are integral membrane proteins responsible for developing resistance against cationic antimicrobial proteins in the majority of the gram-positive bacteria. Studies on *E. faecalis* suggested that mprF2 is essential for the aminoacylation of phosphatidylglycerol (PG) and synthesis of Lys-PG, Ala-PG, and Arg-PG variants. Whereas, mprF1 does not play a role in aminoacylation of PG. Furthermore, the aminoacylation of PG by mprF2 increases resistance against cationic antimicrobial peptides [15]. The strain *E. faecalis* OG1RF circumvent antimicrobial peptides using MprF (Multiple peptide resistance Factors) protein assisted Antimicrobial peptide sensing system by altering the net surface charge of bacterial cell membrane to repel incoming antimicrobial peptides [16].

The peptides targeting Sortase family proteins were identified as potential therapeutics to kill MDR bacterial strains, which is recently an emerging field in the drug discovery process [17]. Hence in this study we performed protein-peptide docking to identify potential biofilm active peptides that can bind to Sortase family protein thereby inhibiting its function. The screened peptides can be further used for designing novel peptide-based therapeutics against MDR *E. faecalis* infection.

Materials and methods

Computational platform

All the computational simulations were carried out on the Linux Mint 18.3 Cinnamon 64-bit platform in Lenovo G50-45 workstation on AMD A8-6410 APU @ 2.00GHz processor. All the software and tools used in this study were open source platforms or free to use for academic purposes.

Primary and secondary structural analysis

The sequence of *E. faecalis* Sortase family protein with accession ID Q836L7 was retrieved from UNIPROT database [18] and its basic sequence information were calculated using ExPASy ProtParam [19]. The physicochemical properties of *Ef*Srt including number of amino acid, molecular weight (Mwt), amino acid composition, theoretical isoelectric point, aliphatic index, *in vitro**in vivo* half-life instability index, and grand average of hydropathicity (GRAVY) were theoretically calculated. The short antibiofilm peptides of length 10-30 were obtained from BaAMPs database [20] and their physico chemical characteristics were calculated using the inbuilt module of BaAMPs database and used for tertiary structure modeling, docking analysis, and energy calculations.

Tertiary structure modelling

The lack of crystallography structural data of E. faecalis Sortase family protein (Q836L7) remained as a bottleneck. Hence we performed homology modeling to depict the 3D structure [21]. The obtained FASTA sequence was used as input to the PSI-BLAST with default parameters to find suitable the template for performing the homology modeling [22]. The best template was selected from suggested templates based on high percentage of sequence identity, query coverage, and valid E-value. The homology modeling was performed using a standalone tool MODELLER v9.21 [23]. The results were ranked based on Discrete Optimized Protein Energy (DOPE) score, the models with least DOPE score were selected and administered to model validation [24]. The modeled 3D structure was refined using Galaxyrefine web server for better quality [25]. The refined 3D coordinates were analyzed for dihedral angles distribution using RAMPAGE web server [26]. Further, refined structure was validated using ProSA web server which provides an overall quality score for a modeled structure based on Cα positions [27]. The reliability of modeled protein was assessed using the Superpose 1.0 web by superimposing the modeled structure of *Ef*Srt with template structure and Root Mean Square Deviation (RMSD) was calculated [28]. The tertiary structure of ligand peptides was designed using CABS-dock [29]. Finally, the tertiary structure of *Ef*Srt and peptides were visualized using Chimera v1.13.1 [30].

Protein-peptide flexible docking

Sortase family proteins (SrtA,B, and C) play an important role in initial attachment of planktonic bacterial cells, and subsequent biofilm formation [31]. In *E. faecalis*, the cell wall anchoring of virulence factors such as aggregation substance and pili were facilitated by Sortase enzymes. Therefore, Sortase family protein (Q836L7) was considered as the docking receptor and the

antibiofilm active peptides were used as ligands. Finally, the receptor protein and peptides were docked using CABS-dock standalone [32]. In CABS-dock the modeled three dimensional structure was used as receptor protein and peptide sequences along with secondary structure data was used as ligand peptides [33]. The CABS-dock performs simulation search for the binding site allowing for full flexibility of the peptide and small fluctuations of the receptor backbone. The CABS-dock protocol consists of the following steps (i) Generating random structures, (ii) Simulation of binding and docking, (iii) Selection of the final representative models, and (iv) Reconstruction of the final models. When protein-peptide docking was performed using CABS-dock with default settings, the structure of the peptide was kept as fully flexible and the structure of the protein receptor was maintained near the initial conformation using soft distance restraints. The soft distance restraints allow small fluctuations of the receptor backbone (1 Å) and large fluctuations of the side chains. Based on the RMSD values of the cluster the top 10 complexes were sorted. The Gibbs free energy (ΔG) and Dissociation constant (Kd) were used to explain the binding strength or potential of the drug-protein complex during drug screening and therapeutics development [34]. Therefore, ΔG and K_d of protein-peptide complexes were predicted using the PRODIGY web server at 37°C [35]. The K_d value of protein-peptide complexes were calculated using ΔG value obtained from PRODIGY using following equation,

$$\Delta G = RT \times \ln K_d \quad \textbf{(1)}$$

where, R, ΔG, and T are the ideal gas constant, gibbs free energy, and temperature (Kelvin), respectively. The binding energy was calculated as follows,

$$\Delta G = -0.09459 \times IC_{charged/charged} - 0.10007 \times IC_{charged/apolar} + 0.19577 \times IC_{polar/polar} - 0.22671 \times IC_{polar/apolar} + 0.18681 \times \%NIS_{apolar} + 0.3810 \times \%NIS_{charged} - 15.9433 \quad \textbf{(2)}$$

where, $IC_{X/Y}$ represents interfacial contacts in terms of physicochemical properties and %NIS represents percentage of non-interacting surfaces in terms of physicochemical properties. The interfacial contacts of protein-peptide complexes were analyzed using COCOMAPS [36] and PPCheck [37] web server and visualized using Chimera v1.13.1.

Non bonded Energy calculation of Protein-peptide complexes

The strength of interactions between protein-protein complexes were calculated using standard energy calculations involving non-bonded interactions like electrostatic, van der Waals, and hydrogen bonds. The hydrogen atoms of protein-peptide complexes were fixed geometrically and then hydrogen bond energy was calculated as follows,

$$E = q1q2\ [1/r(ON) + 1/r(CH) - 1/r(OH) - 1/r(CN)] * 332 * 4.184\ kJ/mol \quad \textbf{(3)}$$

where q1 and q2 are partial atomic charges, r() is the inter-atomic distance between the corresponding atoms. The van der Waals interaction energies are calculated using equation (4)

$$E=4.184\ (E_iE_j) \times [((R_i+R_j)/r)^{12} - 2((R_i+R_j)/r)^{6}]\ KJ/mol \quad \textbf{(4)}$$

where R is the Van der Waals radius for an atom, E is the van der Waals well depth, r is the distance between the atoms. The electrostatic interaction energies for favourable as well as non favourable interactions are calculated according to Coulomb's law by considering the interprotomer charged atomic pairs at ≤10 Å.

Results and Discussion

The antimicrobial peptides were identified as potential alternative therapy to treat MDR bacterial infections. In the past two decades we have identified hundreds of peptides from natural sources and studied their biological activity both *in vivo* and *in vitro* [38]. The studies on antibacterial peptides showed that there is a relationship between structure and functions of these peptides [39]. For example, Members of the defensin family are highly similar in protein sequence but they

show differential antimicrobial activity [40]. Hence it is important to depict the structure-function relationship of these defensin peptides. The cationic antimicrobial peptide Human β-beta defensin 2 disrupts the localization pattern of membrane protein SrtA and SecA in *E. faecalis* [41, 42]. The studies have also proved that the both SrtA and SrtC were focally localized in *E. faecalis* and essential for efficient bacterial colonization and biofilm formation on the host tissue surfaces and was identified as an attractive drug target [43]. We performed protein-peptide flexible docking to identify potential biofilm active peptides that can bind to Sortase family protein thereby inhibiting its function. Also the identified peptide binding *Ef*Srt residues can be considered as potential target sites for the development of potential peptide based therapeutics against biofilm associated infections. Therefore, in this study biofilm active peptides collected from literature sources were screened to investigate its binding mechanism with E. faecalis SrtA.

The primary sequence information of query sequence Q836L7 was theoretically calculated using Expasy ProtParam suggests that the protein has molecular weight (32025.32) and found to be basic (theoretical PI of 9.57), stable (Instability Index < 40), hydrophilic (negative GRAVY value) in nature, and thermostable (higher AI value). Additionally, the half-life was theoretically calculated to be about 30 hours (*in vitro*) in mammalian reticulocytes, >20 hours (*in vivo*) in yeast, and >10 hours (*in vivo*) in *E. coli*. The secondary structural analysis demonstrated the presence of 7.7% helix, 39.4% sheet, 20.6% turn, and 32.3% coil and secondary structure view of modeled structure was illustrated in **Figure 1a**. The physicochemical properties of the peptide ligands were theoretically and depicted in **Table 1**. The length of the peptide ligands ranges from 10-30 AA and showed diverse net charge variation. However, lack of crystallography structural data of *E. faecalis* Sortase family protein (Q836L7) remained as a bottleneck. The PSI-BLAST analysis yielded crystal structure of Sortase C-1 from *Streptococcus pneumoniae* (PDB ID:

w1j.1) with sequence similarity (45.50 %) and sequence coverage (70%) as template for *Ef*Srt [44]. The template structure 2w1j.1 was found to be monomer with resolution of 1.24 Å. The homology modeling was performed using MODELLER v9.21 and the best crude models were selected based on DOPE scores and subjected for structural refinement. The selected crude model was refined using Galaxy Refine web server and validated using PROSA and RAMPAGE web servers. The Z-score of the refined model was found to be -5.92 as compared to -6.87 of crude model which indicated that the structural refinement using Galaxy Refine web server improved the model quality to a greater extent. The Ramachandran plot analysis of refined structure using RAMPAGE web server showed that 146 (95.4%) residues were found in the favored region with 3.3% (5) and 1.3% (2) residues in allowed region and outlier region, respectively. The superposition of template structure and refined model structure was performed using a superpose web server and RMSD was calculated as 1.31 Å and illustrated in **Figure 1b.** The protein-peptide flexible docking was performed using CABS dock standalone package. For docking analysis, the refined model of *Ef*Srt was used as receptor and peptides sequences along with secondary structure information was used as ligand. The CABS dock tool ranks the best protein-peptides based on cluster density, average RMSD, and max RMSD. The binding strength or potential of the best complexes obtained from CABS dock were further evaluated based on the Gibbs free energy (ΔG) and Dissociation constant (Kd) and given in **Table 2**. The ΔG value of peptide-protein complexes ranges from -10.9 to -7.1 $kcal\ mol^{-1}$ and complexes with lowest ΔG values were selected for energy calculations and post docking interaction analysis. The hydrogen bond interaction profile, atom details, distance of peptide-protein complexes were provided in **Table 3**.

Alpha-Defensin-3 is a short peptide of 30 amino acids and molecular weight of 3489.533 Da has three antiparallel beta sheets, covering over 60% of the peptide structure reported to be a role player in innate immunity [45]. Alpha-Defensin-3 has highly stabilized structure due to the presence of three disulfide bridges.

The Alpha-Defensin-3-*Ef*Srt complex showed ΔG and Kd values of -10.9 kcal mol^{-1} and $2.00E^{-08}$ M, respectively. CABS dock results suggested that peptide Alpha-Defensin-3 had better interactions with *Ef*Srt than other peptides with cluster size (24.4929), average RMSD (4.61358), and Maximum RMSD (35.4444). The Alpha-Defensin-3 forms five hydrogen bonds with *Ef*Srt residues at binding interface. The Alpha-Defensin-3 residues ASP1, TYR3, CYS9 were actively involved in hydrogen bonding of average bond length of 2.77 Å (N=5) with *Ef*Srt residues. The atom OH of TYR3 and atom N of ASP 1 were identified as functionally important atoms of Alpha-Defensin-3 peptide for *Ef*Srt binding. The hydrophobic interactions play an important role in peptide-protein binding. Alpha-Defensin-3 forms hydrophobic interactions with residues LEU134 (5.46 Å), LEU134 (6.70 Å), and LEU201 (5.06 Å). The peptide residues ILE6, ALA8, and ALA8 were actively involved in hydrophobic interaction with LEU residues at Alpha-Defensin-3-*Ef*Srt interface. Previous studies on structure activity relationship of defensin peptides suggested that conserved CYS amino acids and associated disulfide bridges were related to its antibacterial activity. The disulfide bonding State and connectivity in the Alpha-Defensin-3 was calculated using the DISULFIND as (2,9) and (4,19). Here we noticed that CYS9 forms disulfide bond with CYS2 and forms hydrogen bond with HIS 202 (2.66 Å) residue of *Ef*Srt. The hydrogen bond interactions between the Alpha-Defensin-3-*Ef*Srt complex was illustrated in **Figure 3d.** The hydrogen bond interaction by disulfide bonding CYS residue may be a unique feature for defensin family peptide and this might be preliminary *in silico* evidence for

contribution of disulfide bridges forming CYS residues towards antibacterial activity of defensin family peptides. Similarly, the residue CYS 15 of a cationic defensin peptide HBD2 forms hydrogen bond of length 3.32 Å with LYS96 residue of *Ef*Srt. HBD2 residue CYS 15 also forms disulfide bonds with CYS30 as shown in **Figure 3a**. The post docking analysis identified four hydrophobic interactions ILE14-TYR98, 24TYR-TYR98, VAL18-TYR139, and PHE19-TYR139.

Pleurocidin is a 2.7 kDa peptide with 25 amino acids which belongs to a family of alpha helical cationic AMP containing amphipathic alpha-helical conformation [46]. This has a broad spectrum antimicrobial activity against Gram positive and Gram negative bacteria with no cytotoxicity toward mammalian cells and low hemolytic activity [46]. The action mechanism of Pleurocidin is translocating strong membrane and pore formation ability with amphipathic helix which reacts with both neutral and acidic anionic phospholipid membranes. Pleurocidin can inhibit nucleic acid and synthesis of protein without the damage of cytoplasmic membranes of *Escherichia coli* at low concentration and at high concentration can potentially kill by causing membrane leakages and causing pore channels [47]. Pleurocidin shows high activity against biofilms *in vitro* [48]. The Pleurocidin-*Ef*Srt complex showed ΔG and Kd values of -10.7 kcal mol^{-1} and $3.00E^{-08}$ M, respectively. The Pleurocidin residues TYR24, VAL16, TYR24, THR22, THR24 were actively involved in hydrogen bonding interaction with residues at Pleurocidin-*Ef*Srt interface as illustrated in **Figure 3c**. The results coincide with previous findings that the antimicrobial activity of pleurocidin is retained in a C-terminal 12-amino acid fragment [49]. The CABS dock results suggested that Pleurocidin-*Ef*Srt had cluster size (56.1134), average RMSD (1.81775), and Maximum RMSD (22.0803). The Pleurocidin forms five hydrogen bonds with *Ef*Srt residues ASP82 (2.58 Å), THR196 (2.61 Å), THR196 (3.43 Å), ARG224 (2.7 Å) at binding interface. The

Pleurocidin residues ALA9, ALA10, TYR24, LEU25, PHE5 were actively involved in hydrophobic interaction with *Ef*Srt interface. Pleurocidin forms hydrophobic interactions with residues PHE84 (5.29 Å), LEU134 (6.99 Å), ILE203 (6.79 Å), ILE220 (6.29 Å), PHE84 (4.81 Å) at *Ef*Srt interface.

Chrysophsin-1, an amphipathic α-helical AMP found in the gill cells of red sea bream. Molecular weight of Chrysophsin-1 is 2892.79 and its hydrophobicity is 48% with a 25-residue peptide. It is a cationic AMP with the capability of broad spectrum bactericidal activity against both gram-positive and gram-negative bacteria [50]. The peptide has broad range activity against bacteria but is more hemolytic compared to other antimicrobial peptides such as Magainin [51]. It is a bioactive peptide that is noted by their unique amino acid compositions such as arginine/lysine-rich peptides. However, histidine-rich bioactive peptides such as Chrysophsin-1 are found rarely [52]. Chrysophsin-1 had a significantly lethal effect on *S. mutans* biofilm by inhibiting the bioactivity of lipopolysaccharide [50]. Three dimensional representation of the best Chrysophsin-1-*Ef*Srt complex was illustrated in **Figure 3b**. CABS dock cluster size, average RMSD, and max RMSD were found to be 25.2909, 8.46153, and 30.1433 respectively. The post docking analysis suggests that the peptide chrysophsin-1 shows a high-binding affinity with *Ef*Srt interface. It forms four hydrogen bond interactions with *Ef*Srt interface residues SER (2.75), GLU100 (2.89), HIS102 (3.22), ASP95 (2.98) as illustrated in **Table 3** and has an ΔG and Kd values of -10.1 kcal mol^{-1} and $7.10E^{-08}$ M, respectively. The chrysophsin-1 forms hydrophobic interactions with *Ef*Srt interface residues ALA124, LEU125, LEU126, LEU127, and LEU156. The Chrysophsin-1 residues ARG23 and ARG24 were identified as potential residues responsible for Chrysophsin-1-*Ef*Srt complex binding.

The strength of interactions between peptide-protein complexes were calculated using standard energy calculations involving non-bonded interactions like electrostatic, van der Waals, and hydrogen bonds. The van der Waals energy, electrostatic energy, hydrogen bond energy, and total stabilizing energy of top four peptide-protein complexes were calculated and presented in **Table 4.** The negative values in energy calculation of top scored complexes shows a good affinity for *Ef*Srt. The total stabilization energy calculation results coincide well with predicted ΔG and Kd values for all top scored complexes. The *Ef*Srt interfacial residues forming hydrogen bonds with peptide ligands were illustrated in **Figure 4**. From standard energy calculation it is evident that van der Waals interactions play an important role in peptide-protein complex formation. In all four peptide-protein complexes studied, the van der Waals interactions contribute most to the binding energy. The results suggest that hydrogen bonds, hydrophobic interactions, and van der Waals interactions helps in molecular recognition by providing specificity and directionality to the protein-peptide complex formation.

Conclusion

This study was performed to identify an effective peptide against *EfSrt* enzyme using protein-peptide flexible docking approach. Detailed inspection on molecular interaction of peptides towards *Ef*Srt enzyme suggests potential residues responsible for peptide-*Ef*Srt enzyme complex formation. Furthermore, we have noticed disulfide bond forming cysteine residues of peptides Alpha-Defensin-3 and HBD2 forms hydrogen bonds with *Ef*Srt enzyme and responsible for peptide-*Ef*Srt enzyme complex formation. similarly, C-terminal 12-amino acids of peptide pleurocidin plays an important role in hydrogen bonding and hydrophobic interactions with *Ef*Srt enzyme. The results provide valuable information at the atomic level for the good binding affinity. In all four peptide-protein complexes studied, the van der Waals interactions contribute

most to the binding energy. The results suggest that hydrogen bonds, hydrophobic interactions, and van der Waals helps in molecular recognition by providing specificity and directionality to the protein-peptide complex formation. However, the peptides identified in this study is the outcome of an in silico protein-peptide flexible docking approach; therefore, it is crucial to prove the proposed hypothesis through experimental validation in both *in vivo* and *in vitro* conditions to prove the efficacy and safety of the identified peptides which may involve the purification of peptides and *Ef*Srt enzyme followed by the crystallization of protein-peptide complex.

References

1. Sivaramakrishnan, M. et al. Screening of curcumin analogues targeting Sortase A enzyme of Enterococcus faecalis: a molecular dynamics approach. *Journal of Proteins and Proteomics* **10**, 245-255 (2019).
2. Ernst, C.M. & Peschel, A. Broad-spectrum antimicrobial peptide resistance by MprF-mediated aminoacylation and flipping of phospholipids. *Molecular microbiology* **80**, 290-299 (2011).
3. Linden, P. & Miller, C. Vancomycin-resistant enterococci: the clinical effect of a common nosocomial pathogen. *Diagnostic microbiology and infectious disease* **33**, 113-120 (1999).
4. Percival, S.L., Suleman, L., Vuotto, C. & Donelli, G. Healthcare-associated infections, medical devices and biofilms: risk, tolerance and control. *Journal of medical microbiology* **64**, 323-334 (2015).
5. Stewart, P.S. et al. Contribution of stress responses to antibiotic tolerance in Pseudomonas aeruginosa biofilms. *Antimicrobial agents and chemotherapy* **59**, 3838-3847 (2015).
6. Comerlato, C.B., Resende, M.C.C.d., Caierão, J. & d'Azevedo, P.A. Presence of virulence factors in Enterococcus faecalis and Enterococcus faecium susceptible and resistant to vancomycin. *Memórias do Instituto Oswaldo Cruz* **108**, 590-595 (2013).
7. Huycke, M.M., Sahm, D.F. & Gilmore, M.S. Multiple-drug resistant enterococci: the nature of the problem and an agenda for the future. *Emerging infectious diseases* **4**, 239 (1998).
8. Anderson, A.C. et al. Enterococcus faecalis from food, clinical specimens, and oral sites: prevalence of virulence factors in association with biofilm formation. *Frontiers in microbiology* **6**, 1534 (2016).
9. Hall, C.W. & Mah, T.-F. Molecular mechanisms of biofilm-based antibiotic resistance and tolerance in pathogenic bacteria. *FEMS microbiology reviews* **41**, 276-301 (2017).
10. Miller, W.R., Munita, J.M. & Arias, C.A. Mechanisms of antibiotic resistance in enterococci. *Expert review of anti-infective therapy* **12**, 1221-1236 (2014).
11. Forrest, G.N. & Tamura, K. Rifampin combination therapy for nonmycobacterial infections. *Clinical microbiology reviews* **23**, 14-34 (2010).

35012. Spirig, T., Weiner, E.M. & Clubb, R.T. Sortase enzymes in Gram-positive bacteria. 351 *Molecular microbiology* **82**, 1044-1059 (2011).
35213. Kline, K.A. et al. Mechanism for sortase localization and the role of sortase localization 353 in efficient pilus assembly in Enterococcus faecalis. *Journal of bacteriology* **191**, 3237- 354 3247 (2009).
35514. Kemp, K.D., Singh, K.V., Nallapareddy, S.R. & Murray, B.E. Relative contributions of 356 Enterococcus faecalis OG1RF sortase-encoding genes, srtA and bps (srtC), to biofilm 357 formation and a murine model of urinary tract infection. *Infection and immunity* **75**, 358 5399-5404 (2007).
35915. Bao, Y. et al. Role of mprF1 and mprF2 in the pathogenicity of Enterococcus faecalis. 360 *PLoS One* **7** (2012).
36116. Rashid, R., Veleba, M. & Kline, K.A. Focal targeting of the bacterial envelope by 362 antimicrobial peptides. *Frontiers in cell and developmental biology* **4**, 55 (2016).
36317. Culp, E. & Wright, G.D. Bacterial proteases, untapped antimicrobial drug targets. *The* 364 *Journal of antibiotics* **70**, 366-377 (2017).
36518. Consortium, U. UniProt: a hub for protein information. *Nucleic acids research* **43**, D204- 366 D212 (2015).
36719. Artimo, P. et al. ExPASy: SIB bioinformatics resource portal. *Nucleic acids research* **40**, 368 W597-W603 (2012).
36920. Di Luca, M., Maccari, G., Maisetta, G. & Batoni, G. BaAMPs: the database of biofilm- 370 active antimicrobial peptides. *Biofouling* **31**, 193-199 (2015).
37121. Cavasotto, C.N. & Phatak, S.S. Homology modeling in drug discovery: current trends 372 and applications. *Drug discovery today* **14**, 676-683 (2009).
37322. Dunbrack Jr, R.L. Comparative modeling of CASP3 targets using PSI-BLAST and 374 SCWRL. *Proteins: Structure, Function, and Bioinformatics* **37**, 81-87 (1999).
37523. Webb, B. & Sali, A. Comparative protein structure modeling using MODELLER. 376 *Current protocols in bioinformatics* **54**, 5.6. 1-5.6. 37 (2016).
37724. Sivaramakrishnan, M. et al. Molecular docking and dynamics studies on plasmepsin V of 378 malarial parasite Plasmodium vivax. *Informatics in Medicine Unlocked*, 100331 (2020).
37925. Heo, L., Park, H. & Seok, C. GalaxyRefine: protein structure refinement driven by side- 380 chain repacking. *Nucleic acids research* **41**, W384-W388 (2013).
38126. Mani, U., Ravisankar, S. & Ramakrishnan, S.M. PDB@: An offline toolkit for 382 exploration and analysis of PDB files. *Journal of structural and functional genomics* **14**, 383 127-133 (2013).
38427. Wiederstein, M. & Sippl, M.J. ProSA-web: interactive web service for the recognition of 385 errors in three-dimensional structures of proteins. *Nucleic acids research* **35**, W407- 386 W410 (2007).
38728. Maiti, R., Van Domselaar, G.H., Zhang, H. & Wishart, D.S. SuperPose: a simple server 388 for sophisticated structural superposition. *Nucleic acids research* **32**, W590-W594 389 (2004).
39029. Blaszczyk, M., Ciemny, M.P., Kolinski, A., Kurcinski, M. & Kmiecik, S. Protein–peptide 391 docking using CABS-dock and contact information. *Briefings in bioinformatics* **20**, 2299- 392 2305 (2019).
39330. Pettersen, E.F. et al. UCSF Chimera—a visualization system for exploratory research and 394 analysis. *Journal of computational chemistry* **25**, 1605-1612 (2004).

39531. Chen, L. & Wen, Y.m. The role of bacterial biofilm in persistent infections and control 396 strategies. *International journal of oral science* **3**, 66-73 (2011).
39732. Kurcinski, M. et al. CABS-dock standalone: a toolbox for flexible protein–peptide 398 docking. *Bioinformatics* **35**, 4170-4172 (2019).
39933. Kurcinski, M., Badaczewska-Dawid, A., Kolinski, M., Kolinski, A. & Kmiecik, S. 400 Flexible docking of peptides to proteins using CABS-dock. *Protein Science* **29**, 211-222 401 (2020).
40234. Hopkins, A.L., Keserü, G.M., Leeson, P.D., Rees, D.C. & Reynolds, C.H. The role of 403 ligand efficiency metrics in drug discovery. *Nature reviews Drug discovery* **13**, 105-121 404 (2014).
40535. Xue, L.C., Rodrigues, J.P., Kastritis, P.L., Bonvin, A.M. & Vangone, A. PRODIGY: a web 406 server for predicting the binding affinity of protein–protein complexes. *Bioinformatics* 407 **32**, 3676-3678 (2016).
40836. Vangone, A., Spinelli, R., Scarano, V., Cavallo, L. & Oliva, R. COCOMAPS: a web 409 application to analyze and visualize contacts at the interface of biomolecular complexes. 410 *Bioinformatics* **27**, 2915-2916 (2011).
41137. Sukhwal, A. & Sowdhamini, R. PPCheck: A webserver for the quantitative analysis of 412 protein-protein interfaces and prediction of residue hotspots. *Bioinformatics and biology* 413 *insights* **9**, BBI. S25928 (2015).
41438. Reddy, K., Yedery, R. & Aranha, C. Antimicrobial peptides: premises and promises. 415 *International journal of antimicrobial agents* **24**, 536-547 (2004).
41639. Powers, J.-P.S. & Hancock, R.E. The relationship between peptide structure and 417 antibacterial activity. *Peptides* **24**, 1681-1691 (2003).
41840. Ganz, T. Defensins: antimicrobial peptides of innate immunity. *Nature reviews* 419 *immunology* **3**, 710-720 (2003).
42041. Kandaswamy, K. et al. Focal targeting by human β-defensin 2 disrupts localized virulence 421 factor assembly sites in Enterococcus faecalis. *Proceedings of the National Academy of* 422 *Sciences* **110**, 20230-20235 (2013).
42342. Gilmore, M.S., Lebreton, F. & Van Tyne, D. Dual defensin strategy for targeting 424 Enterococcus faecalis. *Proceedings of the National Academy of Sciences* **110**, 19980-425 19981 (2013).
42643. Natarajan, G. et al. A big picture on antimicrobial strategies then and now. *Research* 427 *Journal of Engineering and Technology* **8**, 361-364 (2017).
42844. Manzano, C. et al. Sortase-mediated pilus fiber biogenesis in Streptococcus pneumoniae. 429 *Structure* **16**, 1838-1848 (2008).
43045. Hill, C.P., Yee, J., Selsted, M.E. & Eisenberg, D. Crystal structure of defensin HNP-3, an 431 amphiphilic dimer: mechanisms of membrane permeabilization. *Science* **251**, 1481-1485 432 (1991).
43346. Cole, A.M., Weis, P. & Diamond, G. Isolation and characterization of pleurocidin, an 434 antimicrobial peptide in the skin secretions of winter flounder. *Journal of Biological* 435 *Chemistry* **272**, 12008-12013 (1997).
43647. Jorge, P., Lourenco, A. & Pereira, M.O. New trends in peptide-based anti-biofilm 437 strategies: a review of recent achievements and bioinformatic approaches. *Biofouling* **28**, 438 1033-1061 (2012).
43948. Tao, R. et al. Antimicrobial and antibiofilm activity of pleurocidin against cariogenic 440 microorganisms. *Peptides* **32**, 1748-1754 (2011).

44149. Souza, A.L. et al. Antimicrobial activity of pleurocidin is retained in Plc-2, a C-terminal
442 12-amino acid fragment. *Peptides* **45**, 78-84 (2013).
44350. Wang, W. et al. Effect of a novel antimicrobial peptide chrysophsin-1 on oral pathogens
444 and Streptococcus mutans biofilms. *Peptides* **33**, 212-219 (2012).
44551. Mason, A.J. et al. Membrane interaction of chrysophsin-1, a histidine-rich antimicrobial
446 peptide from red sea bream. *Biochemistry* **46**, 15175-15187 (2007).
44752. Tripathi, A.K. et al. Identification of GXXXXG motif in Chrysophsin-1 and its
448 implication in the design of analogs with cell-selective antimicrobial and anti-endotoxin
449 activities. *Scientific reports* **7**, 1-16 (2017).
450

451

452 **Figures**

453

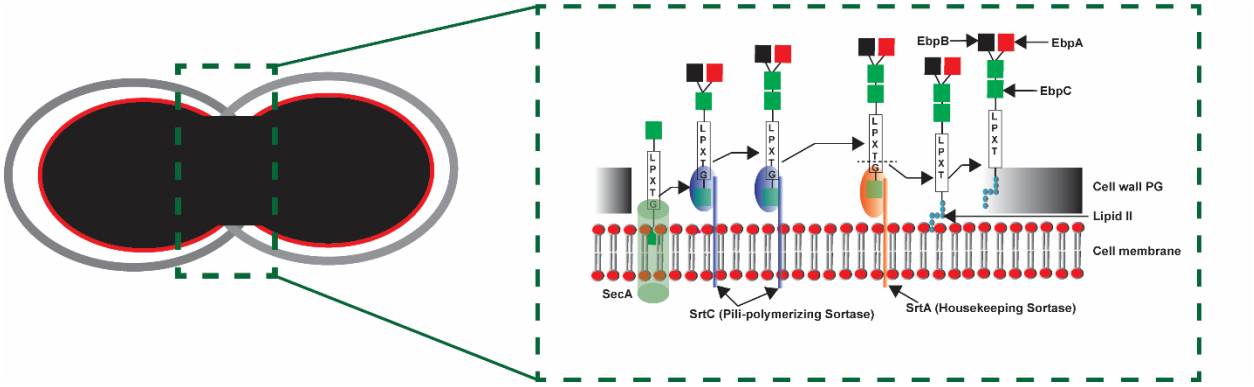

455**Figure 1.** Spatial localization of virulence factors and Sortase mediated pilus assembly in *E.*
456*faecalis*. Endocarditis and biofilm associated pili virulence proteins (EbpA, EbpB, EbpC),
457Sortases (SrtA, SrtC), Peptidoglycan (PG), and universally conserved protein conducting channel
458(SecA).

459

460

461

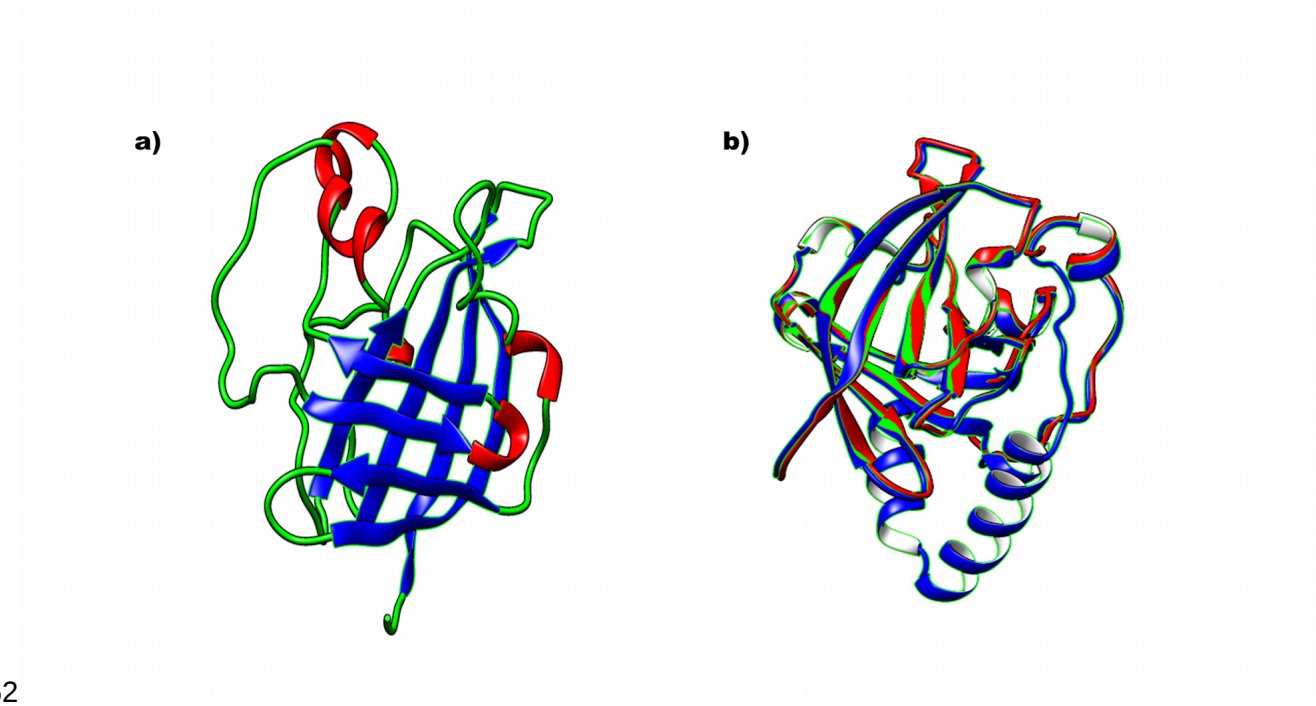

Figure 2. Homology modeling and its structural validation. a) secondary structure of Srt displaying helix (red), beta sheets (blue), and loops (green), b) Superimposition of *Ef*Srt and template structure.

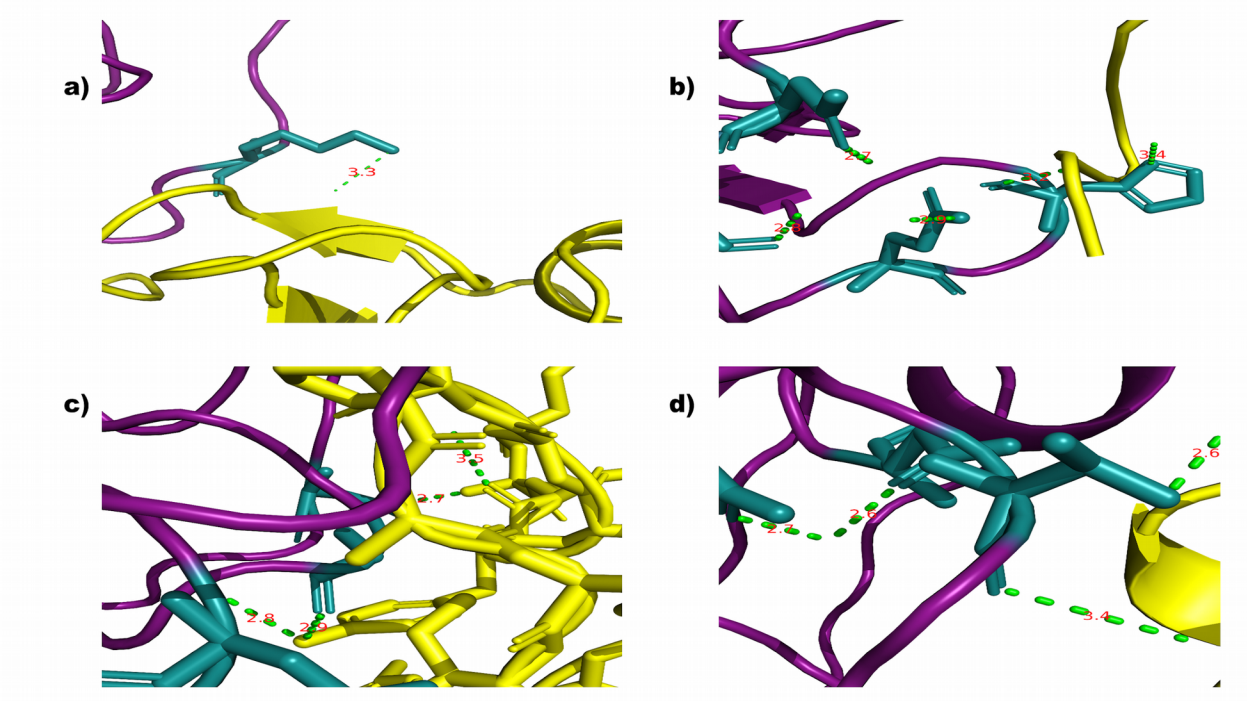

Figure 3. Hydrogen bond interactions between *Ef*Srt and top scored peptides. a) HBD2, b) Chrysophsin-1, c) Pleurocidin, and d) Alpha-Defensin-3.

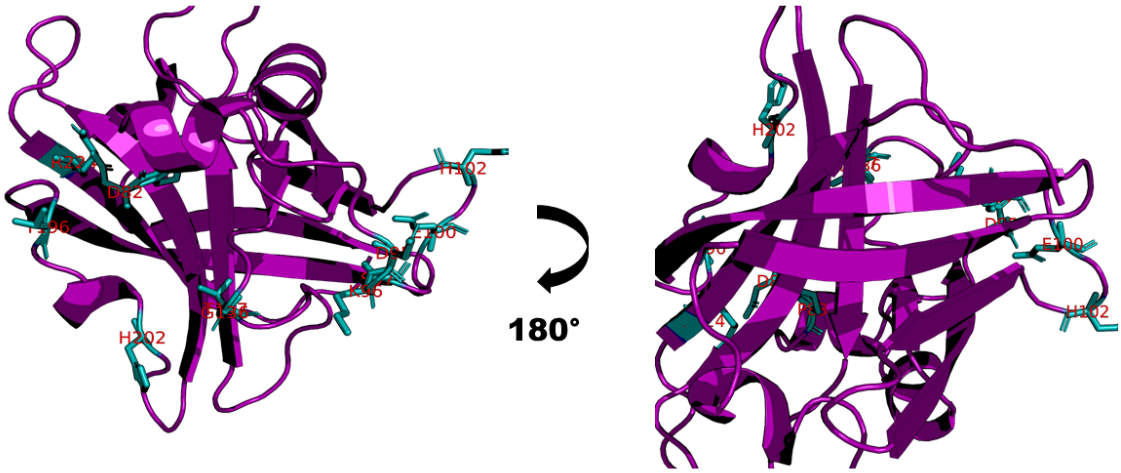

Figure 4. 3D structure of *Ef*Srt (colored in deep purple), on two faces (rotation of 180°). Residues forming hydrogen bonds with peptide ligands are highlighted as sticks and were colored in cyan.

43

494

Tables

Table 1. Physicochemical characteristics of peptides used in this study

Peptides	Size	NetCharge @5	NetCharge @7	Isoelectric Point	Molecular Weight	Hydrophobicity (CCS)	Hydrophobic Mom (CCS)
Lactoferricin (17-30)	14	6.038	5.945	12.263	1922.044	-1.907	1.175
Magainin-I	23	4.119	3.217	10.803	2408.308	-0.378	3.415
Histatin 5	24	12.009	6.657	10.892	3034.519	-4.679	1.436
Pleurocidin	25	6.946	4.695	10.866	2709.47	-0.532	2.147
Chrysophsin-1	25	8.915	5.937	12.813	2890.662	0.24	2.345
BMAP-27	26	11.007	10.215	12.843	3224.047	-0.342	3.554
Melittin B	26	5.038	4.975	12.546	2845.743	-0.015	3.041
BMAP-28	27	7.038	6.975	12.526	3072.932	0.463	3.76
SMAP-29	29	10.007	9.215	3254.036	3254.036	-0.083	3.545
Alpha-Defensin-3	30	1.222	0.853	7.906	2425.85	0.119	1.86

Table 2. Binding energy, Dissociation constant, and cluster properties of peptides against Srt protein of *E. faecalis*

Protein-peptide complex	ΔG (kcal mol^{-1})	Kd (M) at 37.0 °C	Cluster property		
			cluster density	average rmsd	max rmsd
*Ef*Srt-Chrysophsin 1	-10.1	7.10E^{-08}	25.2909	8.46153	30.1433
*Ef*Srt-Magainin I	-9	4.40E^{-07}	26.1185	4.51788	26.6159
*Ef*Srt-Histatin 5	-7.7	4.50E^{-06}	20.4049	6.71407	21.3364
*Ef*Srt-Alpha-Defensin-3	-10.9	2.00E^{-08}	24.4929	4.61358	35.4444
*Ef*Srt-BMAP 27	-7.1	5.90E^{-06}	38.6465	3.77784	30.4999
*Ef*Srt-HBD2	-9.1	1.70E^{-06}	38.9539	5.53975	28.7022
*Ef*Srt-Melittin B	-8.7	7.20E^{-07}	38.8961	2.00534	6.30558
*Ef*Srt-Pleurocidin	-10.7	3.00E^{-08}	56.1134	1.81775	22.0803
*Ef*Srt-SMAP-29	-8.1	1.90E^{-06}	36.5661	3.06294	20.8314

Table 3. Hydrogen bond interactions between the top scored peptides and *E. faecalis* Srt protein

Peptides	Sortase Chain:A				Peptides Chain:B				Bond type and distance	
	Residue Number	Amino Acid	Chain ID	Interacting atoms	Residue Number	Amino Acid	Chain ID	Interacting atoms	Type of H-Bond	Distance (D-A) Å

Chrysophsin-1	97	SER	A	O	24	ARG	B	NH2	BS	2.75
	100	GLU	A	OE2	24	ARG	B	NH1	SS	2.89
	102	HIS	A	O	23	ARG	B	NE	BS	3.22
	95	ASP	A	OD1	24	ARG	B	NE	SS	2.98
Alpha-defensin 3	95	ASP	A	OD1	1	ASP	B	N	SB	2.74
	137	THR	A	O	3	TYR	B	OH	BS	2.83
	136	GLY	A	O	3	TYR	B	OH	SM	2.89
	202	HIS	A	ND1	9	CIS	B	O	SM	2.66
	95	ASP	A	OD1	1	ASP	B	N	MS	2.74
Pleurocidin	224	ARG	A	NH1	24	TYR	B	OH	SS	2.7
	196	THR	A	OG1	16	VAL	B	O	SM	2.61
	82	ASP	A	OD1	24	TYR	B	OH	SS	2.58
	196	THR	A	O	22	THR	B	OG1	SM	3.43
HBD2	96	LYS	A	NZ	15	CYS	B	O	SM	3.32

Table 4. Energy profile of top scored protein-peptide complexes

Protein-peptide complex	**Hydrogen Bond Energy**	**Electrostatic Energy**	**Van der Waals Energy**	**Total Stabilizing Energy**
Chrysophsin 1	-16.99	-40.32	-181.45	-238.76
Alpha-Defensin-3	-17.05	-40.04	-193.32	-250.41
Pleurocidin	-14.13	-14.12	-173.9	-202.15
Human Beta Defensin 2	-10.47	-46.73	-193.47	-250.67

51

519

52

Molecular modeling of structures and interaction of short peptides and Sortase family protein of *Enterococcus faecalis*: Basis for developing peptide-based therapeutics against multidrug resistant strains

Muthusaravanan Sivaramakrishnan [a,b], Kumaravel Kandaswamy [b], Cashlin Anna Suveetha Gnana Rajan [a], Janamitra Arjun [a], Rejoe Raymond [a] and Ram Kothandan *[a].

[a]Bioinformatics Laboratory, Department of Biotechnology, Kumaraguru College of Technology, Coimbatore, Tamil Nadu, India.

[b]Laboratory of Molecular Biology and Genetic Engineering, Department of Biotechnology, Kumaraguru College of Technology, Coimbatore, Tamil Nadu, India.

Graphical abstract

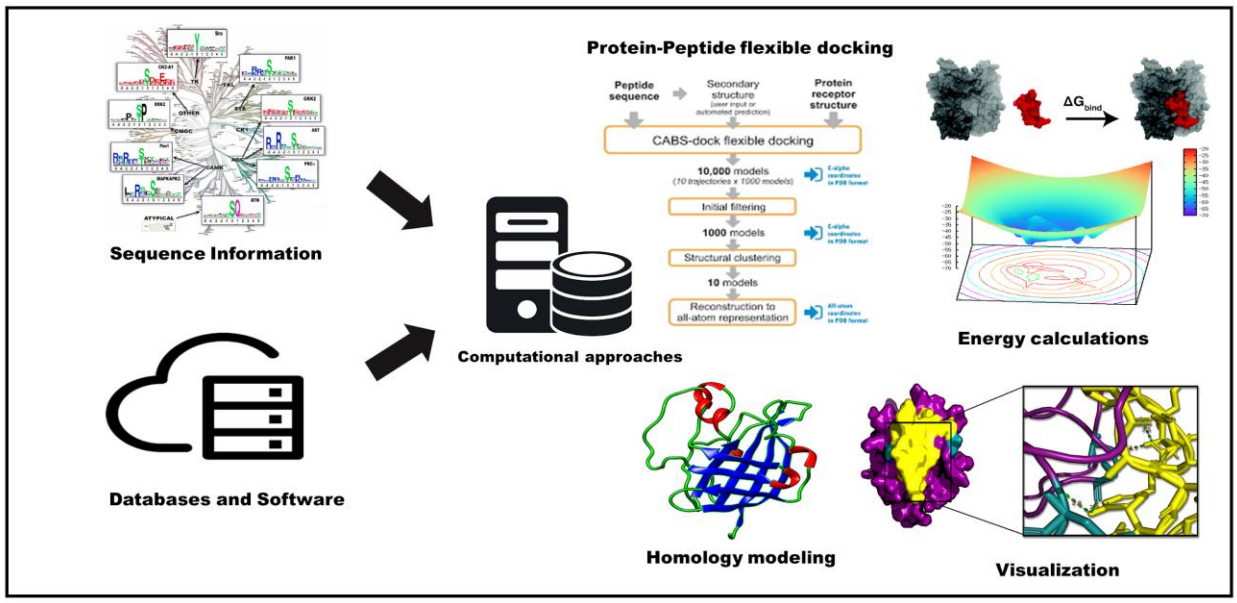

Abstract

The *Enterococcus faecalis* (*E. faecalis*) infection starts with initial adhesion to a host cell or abiotic surface by multiple adhesions on its cell membrane. The pathogenicity is due to virulence factors SrtA, SrtC, EbpA, EbpB, EbpC, and Aggregation Substance. *E. faecalis* developed resistance to the majority of standard therapies. Additionally, a notable key feature of *E. faecalis* is its ability to form biofilm *in vivo*. *E. faecalis* strains show resistance to aminoglycosides and β-lactam antibiotics with different degree of susceptibility. Sortases (SrtA and SrtC) are enzymes spatially localized at the septal region in majority of gram-positive bacteria during the cell cycle, which in-turn plays an important role in proper assembling of adhesive surface proteins and pilus on cell membrane. The studies have also proved that the both SrtA and SrtC were focally localized in *E. faecalis* and essential for efficient bacterial colonization and biofilm formation on the host tissue surfaces Using homology modeling and protein-peptide flexible docking methods, we report here the detailed interaction between peptides and *Ef*Srt (Q836L7) enzyme. Plausible binding modes between *Ef*Srt and the selected short biofilm active peptides were revealed from protein-peptide flexible docking. The simulation data further revealed critical residues at the complex interface and provided more details about the interactions between the peptides and *Ef*Srt. The flexible docking simulations showed that the peptide-*Ef*Srt binding was achieved through hydrogen bonding, hydrophobic, and van der Waals interaction. The strength of interactions between peptide-*Ef*Srt complexes were calculated using standard energy calculations involving non-bonded interactions like electrostatic, van der Waals, and hydrogen bonds.

Keywords: Drug resistance, *E. faecalis*, Biofilm, Sortase enzymes, protein-peptide docking, standard energy calculations.

Introduction

Enterococcus faecalis (*E. faecalis*) is a gram positive commensal opportunistic pathogen, responsible for various hospital acquired infections [1]. *E. faecalis* strains can overcome several harsh environments by forming biofilms on host tissues and abiotic surfaces. Furthermore, *E. faecalis* harbors virulence proteins on its cell membrane and an antimicrobial peptide sensing system to protect them against antibiotics and cationic antimicrobial peptides, respectively [2].

E. faecalis causes over 18,000 deaths a year, making it an important pathogen to be studied. Over the past three decades, various research groups have studied *E. faecalis* strains intensively to explore its interaction with hosts, determine the basis of pathogenesis, and virulence proteins localization to find effective treatment strategies [3]. However, currently there is no effective drug available for its prevention and infections still exist. *E. faecalis* is also capable of forming biofilms and responsible for various biofilm-associated infections such as Urinary Tract Infection (UTI), surgical wound infection, and nosocomial bacteremia [4]. The mature biofilm showed high tolerance to antibiotics than the planktonic bacteria, even at higher concentrations of 10–1000 times [5]. The *E. faecalis* infection starts with initial adhesion to a host cell or abiotic surface by multiple adhesions on its cell membrane. The pathogenicity is due to virulence factors SrtA, SrtC, EbpA, EbpB, EbpC, and Aggregation Substance [6]. *E. faecalis* developed resistance to the majority of standard therapies [7]. Additionally, a notable key feature of *E. faecalis* is its ability to form biofilm [8]. *E. faecalis* strains show resistance to aminoglycosides and β-lactam antibiotics with different degree of susceptibility [9]. It shows moderate resistance to former due to its low permeability through the cell wall (aminoglycoside molecules are larger) and intrinsic resistance to later due to over-expression of penicillin binding proteins. The antibiotics available today were not effective against Multiple Drug Resistance (MDR) enterococcal infections such endocarditis or bacteremia

along with neutropenia [10]. The antibiotics combinations such as ciprofloxacin with ampicillin, novobiocin with doxycycline, and penicillin with vancomycin were used to treat enterococcal infections [11], but efficiency of this treatment remains doubtful.

Sortases (SrtA and SrtC) are enzymes spatially localized at the septal region in majority of gram-positive bacteria during the cell cycle, which in-turn plays an important role in proper assembling of adhesive surface proteins and pilus on cell membrane [12]. The studies have also proved that the both SrtA and SrtC were focally localized in *E. faecalis* and essential for efficient bacterial colonization and biofilm formation on the host tissue surfaces [13]. The Sortase mutants produce defective pili and found to be less virulent than the wild type strain [14]. The Spatial localization of virulence factors and Sortase mediated pilus assembly in *Enterococcus faecalis* was illustrated in **Figure 1**.

Recent studies on antimicrobials suggest that peptides as possible drug candidates and to overcome drug resistance in *E. faecalis*. Moreover, studies have also shown that this species can rapidly acquire resistance even to cationic antimicrobial peptides such as β-beta defensins [15]. Multiple peptide resistance Factors (mprF1 and mprF2) are integral membrane proteins responsible for developing resistance against cationic antimicrobial proteins in the majority of the gram-positive bacteria. Studies on *E. faecalis* suggested that mprF2 is essential for the aminoacylation of phosphatidylglycerol (PG) and synthesis of Lys-PG, Ala-PG, and Arg-PG variants. Whereas, mprF1 does not play a role in aminoacylation of PG. Furthermore, the aminoacylation of PG by mprF2 increases resistance against cationic antimicrobial peptides [15]. The strain *E. faecalis* OG1RF circumvent antimicrobial peptides using MprF (Multiple peptide resistance Factors) protein assisted Antimicrobial peptide sensing system by altering the net surface charge of bacterial cell membrane to repel incoming antimicrobial peptides [16].

The peptides targeting Sortase family proteins were identified as potential therapeutics to kill MDR bacterial strains, which is recently an emerging field in the drug discovery process [17]. Hence in this study we performed protein-peptide docking to identify potential biofilm active peptides that can bind to Sortase family protein thereby inhibiting its function. The screened peptides can be further used for designing novel peptide-based therapeutics against MDR *E. faecalis* infection.

Materials and methods

Computational platform

All the computational simulations were carried out on the Linux Mint 18.3 Cinnamon 64-bit platform in Lenovo G50-45 workstation on AMD A8-6410 APU @ 2.00GHz processor. All the software and tools used in this study were open source platforms or free to use for academic purposes.

Primary and secondary structural analysis

The sequence of *E. faecalis* Sortase family protein with accession ID Q836L7 was retrieved from UNIPROT database [18] and its basic sequence information were calculated using ExPASy ProtParam [19]. The physicochemical properties of *Ef*Srt including number of amino acid, molecular weight (Mwt), amino acid composition, theoretical isoelectric point, aliphatic index, *in vitro**in vivo* half-life instability index, and grand average of hydropathicity (GRAVY) were theoretically calculated. The short antibiofilm peptides of length 10-30 were obtained from BaAMPs database [20] and their physico chemical characteristics were calculated using the inbuilt module of BaAMPs database and used for tertiary structure modeling, docking analysis, and energy calculations.

Tertiary structure modelling

The lack of crystallography structural data of E. faecalis Sortase family protein (Q836L7) remained as a bottleneck. Hence we performed homology modeling to depict the 3D structure [21]. The obtained FASTA sequence was used as input to the PSI-BLAST with default parameters to find suitable the template for performing the homology modeling [22]. The best template was selected from suggested templates based on high percentage of sequence identity, query coverage, and valid E-value. The homology modeling was performed using a standalone tool MODELLER v9.21 [23]. The results were ranked based on Discrete Optimized Protein Energy (DOPE) score, the models with least DOPE score were selected and administered to model validation [24]. The modeled 3D structure was refined using Galaxyrefine web server for better quality [25]. The refined 3D coordinates were analyzed for dihedral angles distribution using RAMPAGE web server [26]. Further, refined structure was validated using ProSA web server which provides an overall quality score for a modeled structure based on Cα positions [27]. The reliability of modeled protein was assessed using the Superpose 1.0 web by superimposing the modeled structure of *Ef*Srt with template structure and Root Mean Square Deviation (RMSD) was calculated [28]. The tertiary structure of ligand peptides was designed using CABS-dock [29]. Finally, the tertiary structure of *Ef*Srt and peptides were visualized using Chimera v1.13.1 [30].

Protein-peptide flexible docking

Sortase family proteins (SrtA,B, and C) play an important role in initial attachment of planktonic bacterial cells, and subsequent biofilm formation [31]. In *E. faecalis*, the cell wall anchoring of virulence factors such as aggregation substance and pili were facilitated by Sortase enzymes. Therefore, Sortase family protein (Q836L7) was considered as the docking receptor and the antibiofilm active peptides were used as ligands. Finally, the receptor protein and peptides were

docked using CABS-dock standalone [32]. In CABS-dock the modeled three dimensional structure was used as receptor protein and peptide sequences along with secondary structure data was used as ligand peptides [33]. The CABS-dock performs simulation search for the binding site allowing for full flexibility of the peptide and small fluctuations of the receptor backbone. The CABS-dock protocol consists of the following steps (i) Generating random structures, (ii) Simulation of binding and docking, (iii) Selection of the final representative models, and (iv) Reconstruction of the final models. When protein-peptide docking was performed using CABS-dock with default settings, the structure of the peptide was kept as fully flexible and the structure of the protein receptor was maintained near the initial conformation using soft distance restraints. The soft distance restraints allow small fluctuations of the receptor backbone (1 Å) and large fluctuations of the side chains. Based on the RMSD values of the cluster the top 10 complexes were sorted. The Gibbs free energy (ΔG) and Dissociation constant (Kd) were used to explain the binding strength or potential of the drug-protein complex during drug screening and therapeutics development [34]. Therefore, ΔG and K_d of protein-peptide complexes were predicted using the PRODIGY web server at 37°C [35]. The K_d value of protein-peptide complexes were calculated using ΔG value obtained from PRODIGY using following equation,

$$\Delta G = RT \times \ln K_d \quad \textbf{(1)}$$

where, R, ΔG, and T are the ideal gas constant, gibbs free energy, and temperature (Kelvin), respectively. The binding energy was calculated as follows,

$$\Delta G = -0.09459 \times IC_{charged/charged} - 0.10007 \times IC_{charged/apolar} + 0.19577 \times IC_{polar/polar} - 0.22671 \times IC_{polar/apolar} + 0.18681 \times \%NIS_{apolar} + 0.3810 \times \%NIS_{charged} - 15.9433 \quad \textbf{(2)}$$

where, $IC_{X/Y}$ represents interfacial contacts in terms of physicochemical properties and %NIS represents percentage of non-interacting surfaces in terms of physicochemical properties. The

interfacial contacts of protein-peptide complexes were analyzed using COCOMAPS [36] and PPCheck [37] web server and visualized using Chimera v1.13.1.

Non bonded Energy calculation of Protein-peptide complexes

The strength of interactions between protein-protein complexes were calculated using standard energy calculations involving non-bonded interactions like electrostatic, van der Waals, and hydrogen bonds. The hydrogen atoms of protein-peptide complexes were fixed geometrically and then hydrogen bond energy was calculated as follows,

$$E = q1q2\ [1/r(ON) + 1/r(CH) - 1/r(OH) - 1/r(CN)] * 332 * 4.184\ kJ/mol \quad \textbf{(3)}$$

where q1 and q2 are partial atomic charges, r() is the inter-atomic distance between the corresponding atoms. The van der Waals interaction energies are calculated using equation (4)

$$E=4.184\ (E_iE_j) \times [((R_i+R_j)/r)^{12} - 2((R_i+R_j)/r)^6]\ KJ/mol \quad \textbf{(4)}$$

where R is the Van der Waals radius for an atom, E is the van der Waals well depth, r is the distance between the atoms. The electrostatic interaction energies for favourable as well as non favourable interactions are calculated according to Coulomb's law by considering the interprotomer charged atomic pairs at ≤10 Å.

Results and Discussion

The antimicrobial peptides were identified as potential alternative therapy to treat MDR bacterial infections. In the past two decades we have identified hundreds of peptides from natural sources and studied their biological activity both *in vivo* and *in vitro* [38]. The studies on antibacterial peptides showed that there is a relationship between structure and functions of these peptides [39]. For example, Members of the defensin family are highly similar in protein sequence but they show differential antimicrobial activity [40]. Hence it is important to depict the structure-function relationship of these defensin peptides. The cationic antimicrobial peptide Human β-beta defensin

2 disrupts the localization pattern of membrane protein SrtA and SecA in *E. faecalis* [41, 42]. The studies have also proved that the both SrtA and SrtC were focally localized in *E. faecalis* and essential for efficient bacterial colonization and biofilm formation on the host tissue surfaces and was identified as an attractive drug target [43]. We performed protein-peptide flexible docking to identify potential biofilm active peptides that can bind to Sortase family protein thereby inhibiting its function. Also the identified peptide binding *Ef*Srt residues can be considered as potential target sites for the development of potential peptide based therapeutics against biofilm associated infections. Therefore, in this study biofilm active peptides collected from literature sources were screened to investigate its binding mechanism with E. faecalis SrtA.

The primary sequence information of query sequence Q836L7 was theoretically calculated using Expasy ProtParam suggests that the protein has molecular weight (32025.32) and found to be basic (theoretical PI of 9.57), stable (Instability Index < 40), hydrophilic (negative GRAVY value) in nature, and thermostable (higher AI value). Additionally, the half-life was theoretically calculated to be about 30 hours (*in vitro*) in mammalian reticulocytes, >20 hours (*in vivo*) in yeast, and >10 hours (*in vivo*) in *E. coli*. The secondary structural analysis demonstrated the presence of 7.7% helix, 39.4% sheet, 20.6% turn, and 32.3% coil and secondary structure view of modeled structure was illustrated in **Figure 1a**. The physicochemical properties of the peptide ligands were theoretically and depicted in **Table 1**. The length of the peptide ligands ranges from 10-30 AA and showed diverse net charge variation. However, lack of crystallography structural data of *E. faecalis* Sortase family protein (Q836L7) remained as a bottleneck. The PSI-BLAST analysis yielded crystal structure of Sortase C-1 from *Streptococcus pneumoniae* (PDB ID: 2w1j.1) with sequence similarity (45.50 %) and sequence coverage (70%) as template for *Ef*Srt [44]. The template structure 2w1j.1 was found to be monomer with resolution of 1.24 Å. The homology modeling was

performed using MODELLER v9.21 and the best crude models were selected based on DOPE scores and subjected for structural refinement. The selected crude model was refined using Galaxy Refine web server and validated using PROSA and RAMPAGE web servers. The Z-score of the refined model was found to be -5.92 as compared to -6.87 of crude model which indicated that the structural refinement using Galaxy Refine web server improved the model quality to a greater extent. The Ramachandran plot analysis of refined structure using RAMPAGE web server showed that 146 (95.4%) residues were found in the favored region with 3.3% (5) and 1.3% (2) residues in allowed region and outlier region, respectively. The superposition of template structure and refined model structure was performed using a superpose web server and RMSD was calculated as 1.31 Å and illustrated in **Figure 1b.**

The protein-peptide flexible docking was performed using CABS dock standalone package. For docking analysis, the refined model of *Ef*Srt was used as receptor and peptides sequences along with secondary structure information was used as ligand. The CABS dock tool ranks the best protein-peptides based on cluster density, average RMSD, and max RMSD. The binding strength or potential of the best complexes obtained from CABS dock were further evaluated based on the Gibbs free energy (ΔG) and Dissociation constant (Kd) and given in **Table 2**. The ΔG value of peptide-protein complexes ranges from -10.9 to -7.1 $kcal\ mol^{-1}$ and complexes with lowest ΔG values were selected for energy calculations and post docking interaction analysis. The hydrogen bond interaction profile, atom details, distance of peptide-protein complexes were provided in **Table 3**. Alpha-Defensin-3 is a short peptide of 30 amino acids and molecular weight of 3489.533 Da has three antiparallel beta sheets, covering over 60% of the peptide structure reported to be a role player in innate immunity [45]. Alpha-Defensin-3 has highly stabilized structure due to the presence of three disulfide bridges.

The Alpha-Defensin-3-*Ef*Srt complex showed ΔG and Kd values of -10.9 kcal mol^{-1} and $2.00E^{-08}$ M, respectively. CABS dock results suggested that peptide Alpha-Defensin-3 had better interactions with *Ef*Srt than other peptides with cluster size (24.4929), average RMSD (4.61358), and Maximum RMSD (35.4444). The Alpha-Defensin-3 forms five hydrogen bonds with *Ef*Srt residues at binding interface. The Alpha-Defensin-3 residues ASP1, TYR3, CYS9 were actively involved in hydrogen bonding of average bond length of 2.77 Å (N=5) with *Ef*Srt residues. The atom OH of TYR3 and atom N of ASP 1 were identified as functionally important atoms of Alpha-Defensin-3 peptide for *Ef*Srt binding. The hydrophobic interactions play an important role in peptide-protein binding. Alpha-Defensin-3 forms hydrophobic interactions with residues LEU134 (5.46 Å), LEU134 (6.70 Å), and LEU201 (5.06 Å). The peptide residues ILE6, ALA8, and ALA8 were actively involved in hydrophobic interaction with LEU residues at Alpha-Defensin-3-*Ef*Srt interface. Previous studies on structure activity relationship of defensin peptides suggested that conserved CYS amino acids and associated disulfide bridges were related to its antibacterial activity. The disulfide bonding State and connectivity in the Alpha-Defensin-3 was calculated using the DISULFIND as (2,9) and (4,19). Here we noticed that CYS9 forms disulfide bond with CYS2 and forms hydrogen bond with HIS 202 (2.66 Å) residue of *Ef*Srt. The hydrogen bond interactions between the Alpha-Defensin-3-*Ef*Srt complex was illustrated in **Figure 3d.** The hydrogen bond interaction by disulfide bonding CYS residue may be a unique feature for defensin family peptide and this might be preliminary *in silico* evidence for contribution of disulfide bridges forming CYS residues towards antibacterial activity of defensin family peptides. Similarly, the residue CYS 15 of a cationic defensin peptide HBD2 forms hydrogen bond of length 3.32 Å with LYS96 residue of *Ef*Srt. HBD2 residue CYS 15 also forms disulfide bonds with CYS30 as shown

in **Figure 3a**. The post docking analysis identified four hydrophobic interactions ILE14-TYR98, 24TYR-TYR98, VAL18-TYR139, and PHE19-TYR139.

Pleurocidin is a 2.7 kDa peptide with 25 amino acids which belongs to a family of alpha helical cationic AMP containing amphipathic alpha-helical conformation [46]. This has a broad spectrum antimicrobial activity against Gram positive and Gram negative bacteria with no cytotoxicity toward mammalian cells and low hemolytic activity [46]. The action mechanism of Pleurocidin is translocating strong membrane and pore formation ability with amphipathic helix which reacts with both neutral and acidic anionic phospholipid membranes. Pleurocidin can inhibit nucleic acid and synthesis of protein without the damage of cytoplasmic membranes of *Escherichia coli* at low concentration and at high concentration can potentially kill by causing membrane leakages and causing pore channels [47]. Pleurocidin shows high activity against biofilms *in vitro* [48]. The Pleurocidin-*Ef*Srt complex showed ΔG and Kd values of -10.7 kcal mol^{-1} and $3.00E^{-08}$ M, respectively. The Pleurocidin residues TYR24, VAL16, TYR24, THR22, THR24 were actively involved in hydrogen bonding interaction with residues at Pleurocidin-*Ef*Srt interface as illustrated in **Figure 3c**. The results coincide with previous findings that the antimicrobial activity of pleurocidin is retained in a C-terminal 12-amino acid fragment [49]. The CABS dock results suggested that Pleurocidin-*Ef*Srt had cluster size (56.1134), average RMSD (1.81775), and Maximum RMSD (22.0803). The Pleurocidin forms five hydrogen bonds with *Ef*Srt residues ASP82 (2.58 Å), THR196 (2.61 Å), THR196 (3.43 Å), ARG224 (2.7 Å) at binding interface. The Pleurocidin residues ALA9, ALA10, TYR24, LEU25, PHE5 were actively involved in hydrophobic interaction with *Ef*Srt interface. Pleurocidin forms hydrophobic interactions with residues PHE84 (5.29 Å), LEU134 (6.99 Å), ILE203 (6.79 Å), ILE220 (6.29 Å), PHE84 (4.81 Å) at *Ef*Srt interface.

Chrysophsin-1, an amphipathic α-helical AMP found in the gill cells of red sea bream. Molecular weight of Chrysophsin-1 is 2892.79 and its hydrophobicity is 48% with a 25-residue peptide. It is a cationic AMP with the capability of broad spectrum bactericidal activity against both gram-positive and gram-negative bacteria [50]. The peptide has broad range activity against bacteria but is more hemolytic compared to other antimicrobial peptides such as Magainin [51]. It is a bioactive peptide that is noted by their unique amino acid compositions such as arginine/lysine-rich peptides. However, histidine-rich bioactive peptides such as Chrysophsin-1 are found rarely [52]. Chrysophsin-1 had a significantly lethal effect on *S. mutans* biofilm by inhibiting the bioactivity of lipopolysaccharide [50]. Three dimensional representation of the best Chrysophsin-1-*Ef*Srt complex was illustrated in **Figure 3b**. CABS dock cluster size, average RMSD, and max RMSD were found to be 25.2909, 8.46153, and 30.1433 respectively. The post docking analysis suggests that the peptide chrysophsin-1 shows a high-binding affinity with *Ef*Srt interface. It forms four hydrogen bond interactions with *Ef*Srt interface residues SER (2.75), GLU100 (2.89), HIS102 (3.22), ASP95 (2.98) as illustrated in **Table 3** and has an ΔG and Kd values of -10.1 kcal mol^{-1} and $7.10E^{-08}$ M, respectively. The chrysophsin-1 forms hydrophobic interactions with *Ef*Srt interface residues ALA124, LEU125, LEU126, LEU127, and LEU156. The Chrysophsin-1 residues ARG23 and ARG24 were identified as potential residues responsible for Chrysophsin-1-*Ef*Srt complex binding.

The strength of interactions between peptide-protein complexes were calculated using standard energy calculations involving non-bonded interactions like electrostatic, van der Waals, and hydrogen bonds. The van der Waals energy, electrostatic energy, hydrogen bond energy, and total stabilizing energy of top four peptide-protein complexes were calculated and presented in **Table**

4. The negative values in energy calculation of top scored complexes shows a good affinity for *Ef*Srt. The total stabilization energy calculation results coincide well with predicted ΔG and Kd values for all top scored complexes. The *Ef*Srt interfacial residues forming hydrogen bonds with peptide ligands were illustrated in **Figure 4**. From standard energy calculation it is evident that van der Waals interactions play an important role in peptide-protein complex formation. In all four peptide-protein complexes studied, the van der Waals interactions contribute most to the binding energy. The results suggest that hydrogen bonds, hydrophobic interactions, and van der Waals interactions helps in molecular recognition by providing specificity and directionality to the protein-peptide complex formation.

Conclusion

This study was performed to identify an effective peptide against *EfSrt* enzyme using protein-peptide flexible docking approach. Detailed inspection on molecular interaction of peptides towards *Ef*Srt enzyme suggests potential residues responsible for peptide-*Ef*Srt enzyme complex formation. Furthermore, we have noticed disulfide bond forming cysteine residues of peptides Alpha-Defensin-3 and HBD2 forms hydrogen bonds with *Ef*Srt enzyme and responsible for peptide-*Ef*Srt enzyme complex formation. similarly, C-terminal 12-amino acids of peptide pleurocidin plays an important role in hydrogen bonding and hydrophobic interactions with *Ef*Srt enzyme. The results provide valuable information at the atomic level for the good binding affinity. In all four peptide-protein complexes studied, the van der Waals interactions contribute most to the binding energy. The results suggest that hydrogen bonds, hydrophobic interactions, and van der Waals helps in molecular recognition by providing specificity and directionality to the protein-peptide complex formation. However, the peptides identified in this study is the outcome of an in silico protein-peptide flexible docking approach; therefore, it is crucial to prove the proposed

hypothesis through experimental validation in both *in vivo* and *in vitro* conditions to prove the efficacy and safety of the identified peptides which may involve the purification of peptides and *Ef*Srt enzyme followed by the crystallization of protein-peptide complex.

References

1. Sivaramakrishnan, M. et al. Screening of curcumin analogues targeting Sortase A enzyme of Enterococcus faecalis: a molecular dynamics approach. *Journal of Proteins and Proteomics* **10**, 245-255 (2019).
2. Ernst, C.M. & Peschel, A. Broad-spectrum antimicrobial peptide resistance by MprF-mediated aminoacylation and flipping of phospholipids. *Molecular microbiology* **80**, 290-299 (2011).
3. Linden, P. & Miller, C. Vancomycin-resistant enterococci: the clinical effect of a common nosocomial pathogen. *Diagnostic microbiology and infectious disease* **33**, 113-120 (1999).
4. Percival, S.L., Suleman, L., Vuotto, C. & Donelli, G. Healthcare-associated infections, medical devices and biofilms: risk, tolerance and control. *Journal of medical microbiology* **64**, 323-334 (2015).
5. Stewart, P.S. et al. Contribution of stress responses to antibiotic tolerance in Pseudomonas aeruginosa biofilms. *Antimicrobial agents and chemotherapy* **59**, 3838-3847 (2015).
6. Comerlato, C.B., Resende, M.C.C.d., Caierão, J. & d'Azevedo, P.A. Presence of virulence factors in Enterococcus faecalis and Enterococcus faecium susceptible and resistant to vancomycin. *Memórias do Instituto Oswaldo Cruz* **108**, 590-595 (2013).
7. Huycke, M.M., Sahm, D.F. & Gilmore, M.S. Multiple-drug resistant enterococci: the nature of the problem and an agenda for the future. *Emerging infectious diseases* **4**, 239 (1998).
8. Anderson, A.C. et al. Enterococcus faecalis from food, clinical specimens, and oral sites: prevalence of virulence factors in association with biofilm formation. *Frontiers in microbiology* **6**, 1534 (2016).
9. Hall, C.W. & Mah, T.-F. Molecular mechanisms of biofilm-based antibiotic resistance and tolerance in pathogenic bacteria. *FEMS microbiology reviews* **41**, 276-301 (2017).
10. Miller, W.R., Munita, J.M. & Arias, C.A. Mechanisms of antibiotic resistance in enterococci. *Expert review of anti-infective therapy* **12**, 1221-1236 (2014).
11. Forrest, G.N. & Tamura, K. Rifampin combination therapy for nonmycobacterial infections. *Clinical microbiology reviews* **23**, 14-34 (2010).
12. Spirig, T., Weiner, E.M. & Clubb, R.T. Sortase enzymes in Gram-positive bacteria. *Molecular microbiology* **82**, 1044-1059 (2011).
13. Kline, K.A. et al. Mechanism for sortase localization and the role of sortase localization in efficient pilus assembly in Enterococcus faecalis. *Journal of bacteriology* **191**, 3237-3247 (2009).
14. Kemp, K.D., Singh, K.V., Nallapareddy, S.R. & Murray, B.E. Relative contributions of Enterococcus faecalis OG1RF sortase-encoding genes, srtA and bps (srtC), to biofilm formation and a murine model of urinary tract infection. *Infection and immunity* **75**, 5399-5404 (2007).

15. Bao, Y. et al. Role of mprF1 and mprF2 in the pathogenicity of Enterococcus faecalis. *PLoS One* **7** (2012).
16. Rashid, R., Veleba, M. & Kline, K.A. Focal targeting of the bacterial envelope by antimicrobial peptides. *Frontiers in cell and developmental biology* **4**, 55 (2016).
17. Culp, E. & Wright, G.D. Bacterial proteases, untapped antimicrobial drug targets. *The Journal of antibiotics* **70**, 366-377 (2017).
18. Consortium, U. UniProt: a hub for protein information. *Nucleic acids research* **43**, D204-D212 (2015).
19. Artimo, P. et al. ExPASy: SIB bioinformatics resource portal. *Nucleic acids research* **40**, W597-W603 (2012).
20. Di Luca, M., Maccari, G., Maisetta, G. & Batoni, G. BaAMPs: the database of biofilm-active antimicrobial peptides. *Biofouling* **31**, 193-199 (2015).
21. Cavasotto, C.N. & Phatak, S.S. Homology modeling in drug discovery: current trends and applications. *Drug discovery today* **14**, 676-683 (2009).
22. Dunbrack Jr, R.L. Comparative modeling of CASP3 targets using PSI-BLAST and SCWRL. *Proteins: Structure, Function, and Bioinformatics* **37**, 81-87 (1999).
23. Webb, B. & Sali, A. Comparative protein structure modeling using MODELLER. *Current protocols in bioinformatics* **54**, 5.6. 1-5.6. 37 (2016).
24. Sivaramakrishnan, M. et al. Molecular docking and dynamics studies on plasmepsin V of malarial parasite Plasmodium vivax. *Informatics in Medicine Unlocked*, 100331 (2020).
25. Heo, L., Park, H. & Seok, C. GalaxyRefine: protein structure refinement driven by side-chain repacking. *Nucleic acids research* **41**, W384-W388 (2013).
26. Mani, U., Ravisankar, S. & Ramakrishnan, S.M. PDB@: An offline toolkit for exploration and analysis of PDB files. *Journal of structural and functional genomics* **14**, 127-133 (2013).
27. Wiederstein, M. & Sippl, M.J. ProSA-web: interactive web service for the recognition of errors in three-dimensional structures of proteins. *Nucleic acids research* **35**, W407-W410 (2007).
28. Maiti, R., Van Domselaar, G.H., Zhang, H. & Wishart, D.S. SuperPose: a simple server for sophisticated structural superposition. *Nucleic acids research* **32**, W590-W594 (2004).
29. Blaszczyk, M., Ciemny, M.P., Kolinski, A., Kurcinski, M. & Kmiecik, S. Protein–peptide docking using CABS-dock and contact information. *Briefings in bioinformatics* **20**, 2299-2305 (2019).
30. Pettersen, E.F. et al. UCSF Chimera—a visualization system for exploratory research and analysis. *Journal of computational chemistry* **25**, 1605-1612 (2004).
31. Chen, L. & Wen, Y.m. The role of bacterial biofilm in persistent infections and control strategies. *International journal of oral science* **3**, 66-73 (2011).
32. Kurcinski, M. et al. CABS-dock standalone: a toolbox for flexible protein–peptide docking. *Bioinformatics* **35**, 4170-4172 (2019).
33. Kurcinski, M., Badaczewska-Dawid, A., Kolinski, M., Kolinski, A. & Kmiecik, S. Flexible docking of peptides to proteins using CABS-dock. *Protein Science* **29**, 211-222 (2020).
34. Hopkins, A.L., Keserü, G.M., Leeson, P.D., Rees, D.C. & Reynolds, C.H. The role of ligand efficiency metrics in drug discovery. *Nature reviews Drug discovery* **13**, 105-121 (2014).

35. Xue, L.C., Rodrigues, J.P., Kastritis, P.L., Bonvin, A.M. & Vangone, A. PRODIGY: a web server for predicting the binding affinity of protein–protein complexes. *Bioinformatics* **32**, 3676-3678 (2016).
36. Vangone, A., Spinelli, R., Scarano, V., Cavallo, L. & Oliva, R. COCOMAPS: a web application to analyze and visualize contacts at the interface of biomolecular complexes. *Bioinformatics* **27**, 2915-2916 (2011).
37. Sukhwal, A. & Sowdhamini, R. PPCheck: A webserver for the quantitative analysis of protein-protein interfaces and prediction of residue hotspots. *Bioinformatics and biology insights* **9**, BBI. S25928 (2015).
38. Reddy, K., Yedery, R. & Aranha, C. Antimicrobial peptides: premises and promises. *International journal of antimicrobial agents* **24**, 536-547 (2004).
39. Powers, J.-P.S. & Hancock, R.E. The relationship between peptide structure and antibacterial activity. *Peptides* **24**, 1681-1691 (2003).
40. Ganz, T. Defensins: antimicrobial peptides of innate immunity. *Nature reviews immunology* **3**, 710-720 (2003).
41. Kandaswamy, K. et al. Focal targeting by human β-defensin 2 disrupts localized virulence factor assembly sites in Enterococcus faecalis. *Proceedings of the National Academy of Sciences* **110**, 20230-20235 (2013).
42. Gilmore, M.S., Lebreton, F. & Van Tyne, D. Dual defensin strategy for targeting Enterococcus faecalis. *Proceedings of the National Academy of Sciences* **110**, 19980-19981 (2013).
43. Natarajan, G. et al. A big picture on antimicrobial strategies then and now. *Research Journal of Engineering and Technology* **8**, 361-364 (2017).
44. Manzano, C. et al. Sortase-mediated pilus fiber biogenesis in Streptococcus pneumoniae. *Structure* **16**, 1838-1848 (2008).
45. Hill, C.P., Yee, J., Selsted, M.E. & Eisenberg, D. Crystal structure of defensin HNP-3, an amphiphilic dimer: mechanisms of membrane permeabilization. *Science* **251**, 1481-1485 (1991).
46. Cole, A.M., Weis, P. & Diamond, G. Isolation and characterization of pleurocidin, an antimicrobial peptide in the skin secretions of winter flounder. *Journal of Biological Chemistry* **272**, 12008-12013 (1997).
47. Jorge, P., Lourenco, A. & Pereira, M.O. New trends in peptide-based anti-biofilm strategies: a review of recent achievements and bioinformatic approaches. *Biofouling* **28**, 1033-1061 (2012).
48. Tao, R. et al. Antimicrobial and antibiofilm activity of pleurocidin against cariogenic microorganisms. *Peptides* **32**, 1748-1754 (2011).
49. Souza, A.L. et al. Antimicrobial activity of pleurocidin is retained in Plc-2, a C-terminal 12-amino acid fragment. *Peptides* **45**, 78-84 (2013).
50. Wang, W. et al. Effect of a novel antimicrobial peptide chrysophsin-1 on oral pathogens and Streptococcus mutans biofilms. *Peptides* **33**, 212-219 (2012).
51. Mason, A.J. et al. Membrane interaction of chrysophsin-1, a histidine-rich antimicrobial peptide from red sea bream. *Biochemistry* **46**, 15175-15187 (2007).
52. Tripathi, A.K. et al. Identification of GXXXXG motif in Chrysophsin-1 and its implication in the design of analogs with cell-selective antimicrobial and anti-endotoxin activities. *Scientific reports* **7**, 1-16 (2017).

Figures

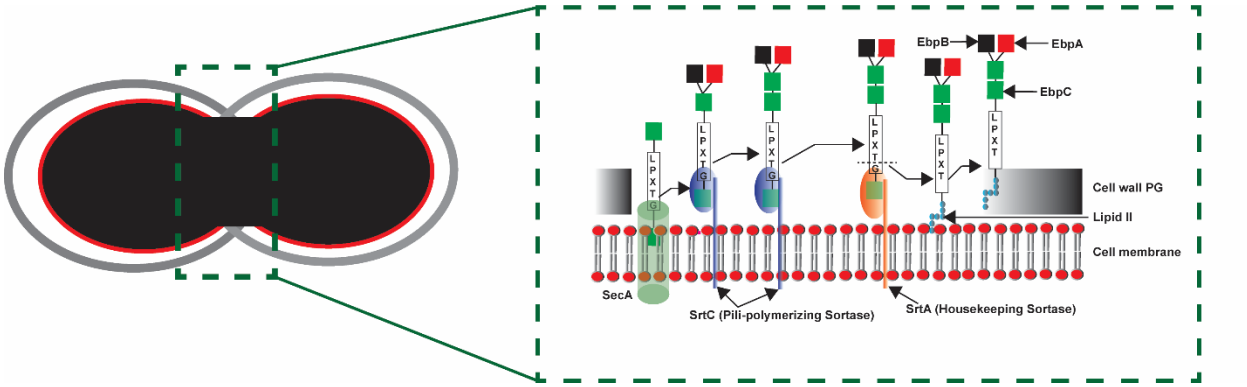

Figure 1. Spatial localization of virulence factors and Sortase mediated pilus assembly in *E. faecalis*. Endocarditis and biofilm associated pili virulence proteins (EbpA, EbpB, EbpC), Sortases (SrtA, SrtC), Peptidoglycan (PG), and universally conserved protein conducting channel (SecA).

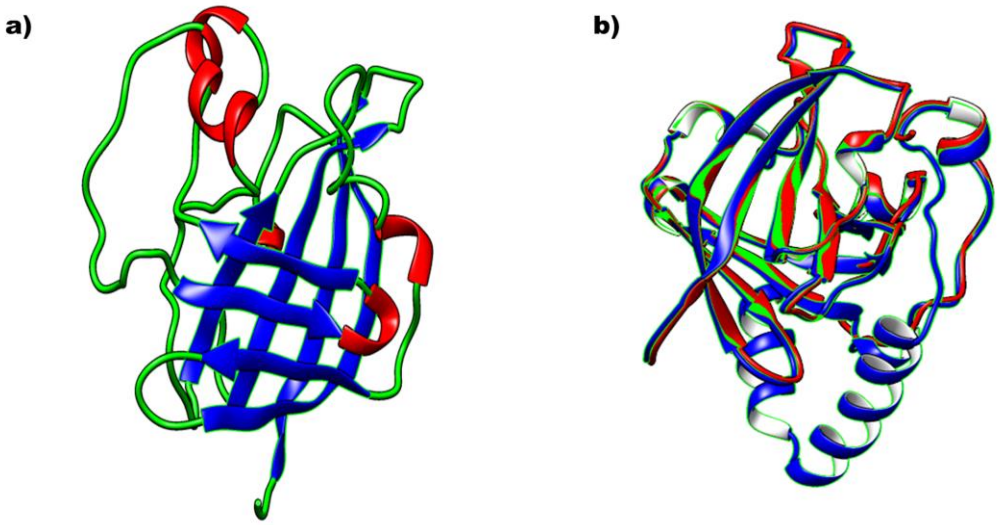

Figure 2. Homology modeling and its structural validation. a) secondary structure of Srt displaying helix (red), beta sheets (blue), and loops (green), b) Superimposition of *Ef*Srt and template structure.

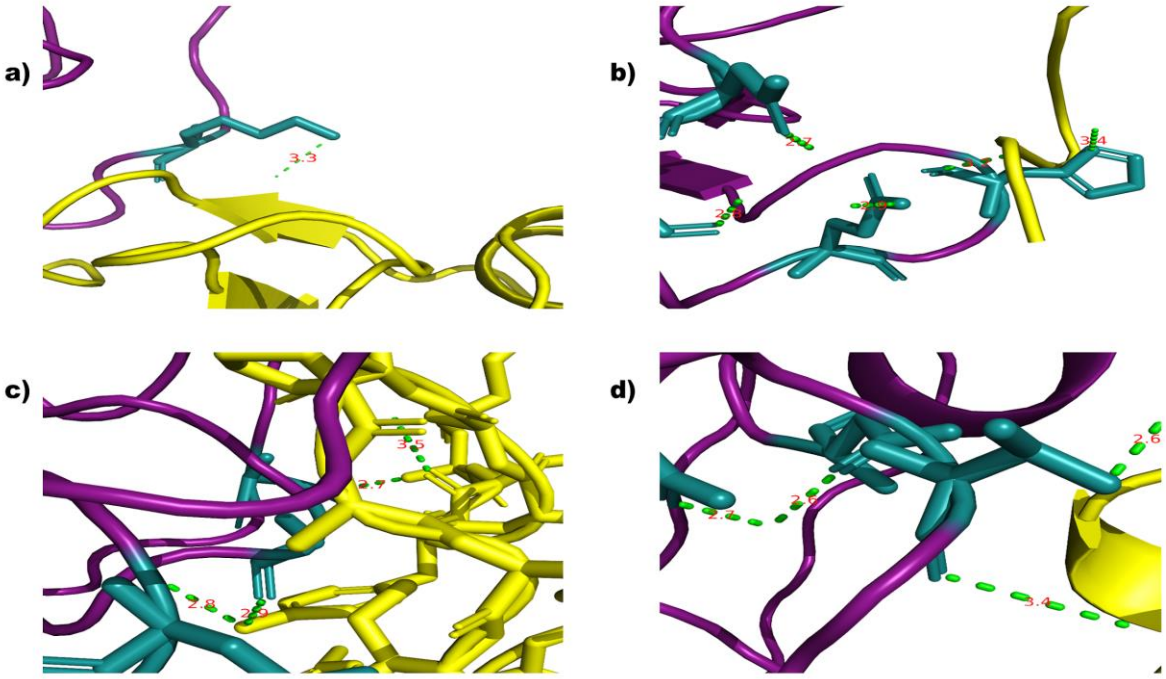

Figure 3. Hydrogen bond interactions between *Ef*Srt and top scored peptides. a) HBD2, b) Chrysophsin-1, c) Pleurocidin, and d) Alpha-Defensin-3.

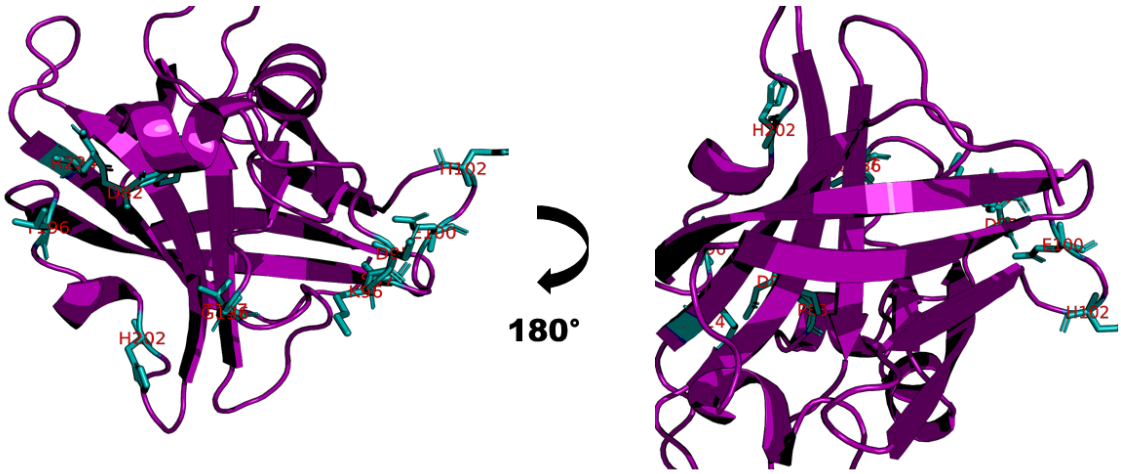

Figure 4. 3D structure of *Ef*Srt (colored in deep purple), on two faces (rotation of 180°). Residues forming hydrogen bonds with peptide ligands are highlighted as sticks and were colored in cyan.

Tables

Table 1. Physicochemical characteristics of peptides used in this study

Peptides	Size	NetCharge @5	NetCharge @7	Isoelectric Point	Molecular Weight	Hydrophobicity (CCS)	Hydrophobic Mom (CCS)
Lactoferricin (17-30)	14	6.038	5.945	12.263	1922.044	-1.907	1.175
Magainin-I	23	4.119	3.217	10.803	2408.308	-0.378	3.415
Histatin 5	24	12.009	6.657	10.892	3034.519	-4.679	1.436
Pleurocidin	25	6.946	4.695	10.866	2709.47	-0.532	2.147
Chrysophsin-1	25	8.915	5.937	12.813	2890.662	0.24	2.345
BMAP-27	26	11.007	10.215	12.843	3224.047	-0.342	3.554
Melittin B	26	5.038	4.975	12.546	2845.743	-0.015	3.041
BMAP-28	27	7.038	6.975	12.526	3072.932	0.463	3.76
SMAP-29	29	10.007	9.215	3254.036	3254.036	-0.083	3.545
Alpha-Defensin-3	30	1.222	0.853	7.906	2425.85	0.119	1.86

Table 2. Binding energy, Dissociation constant, and cluster properties of peptides against Srt protein of *E. faecalis*

Protein-peptide complex	ΔG (kcal mol^{-1})	Kd (M) at 37.0 ℃	Cluster property		
			cluster density	average rmsd	max rmsd
*Ef*Srt-Chrysophsin 1	-10.1	$7.10E^{-08}$	25.2909	8.46153	30.1433
*Ef*Srt-Magainin I	-9	$4.40E^{-07}$	26.1185	4.51788	26.6159
*Ef*Srt-Histatin 5	-7.7	$4.50E^{-06}$	20.4049	6.71407	21.3364
*Ef*Srt-Alpha-Defensin-3	-10.9	$2.00E^{-08}$	24.4929	4.61358	35.4444
*Ef*Srt-BMAP 27	-7.1	$5.90E^{-06}$	38.6465	3.77784	30.4999
*Ef*Srt-HBD2	-9.1	$1.70E^{-06}$	38.9539	5.53975	28.7022
*Ef*Srt-Melittin B	-8.7	$7.20E^{-07}$	38.8961	2.00534	6.30558
*Ef*Srt-Pleurocidin	-10.7	$3.00E^{-08}$	56.1134	1.81775	22.0803
*Ef*Srt-SMAP-29	-8.1	$1.90E^{-06}$	36.5661	3.06294	20.8314

Table 3. Hydrogen bond interactions between the top scored peptides and *E. faecalis* Srt protein

Peptides	Sortase Chain:A				Peptides Chain:B				Bond type and distance	
	Residue Number	**Amino Acid**	**Chain ID**	**Interacting atoms**	**Residue Number**	**Amino Acid**	**Chain ID**	**Interacting atoms**	**Type of H-Bond**	**Distance (D-A) Å**
Chrysophsin-1	97	SER	A	O	24	ARG	B	NH2	BS	2.75
	100	GLU	A	OE2	24	ARG	B	NH1	SS	2.89
	102	HIS	A	O	23	ARG	B	NE	BS	3.22
	95	ASP	A	OD1	24	ARG	B	NE	SS	2.98
Alpha-defensin 3	95	ASP	A	OD1	1	ASP	B	N	SB	2.74
	137	THR	A	O	3	TYR	B	OH	BS	2.83
	136	GLY	A	O	3	TYR	B	OH	SM	2.89
	202	HIS	A	ND1	9	CIS	B	O	SM	2.66
	95	ASP	A	OD1	1	ASP	B	N	MS	2.74
Pleurocidin	224	ARG	A	NH1	24	TYR	B	OH	SS	2.7
	196	THR	A	OG1	16	VAL	B	O	SM	2.61
	82	ASP	A	OD1	24	TYR	B	OH	SS	2.58
	196	THR	A	O	22	THR	B	OG1	SM	3.43
HBD2	96	LYS	A	NZ	15	CYS	B	O	SM	3.32

Table 4. Energy profile of top scored protein-peptide complexes

Protein-peptide complex	**Hydrogen Bond Energy**	**Electrostatic Energy**	**Van der Waals Energy**	**Total Stabilizing Energy**
Chrysophsin 1	-16.99	-40.32	-181.45	-238.76
Alpha-Defensin-3	-17.05	-40.04	-193.32	-250.41
Pleurocidin	-14.13	-14.12	-173.9	-202.15
Human Beta Defensin 2	-10.47	-46.73	-193.47	-250.67